Fluorescent Probes with FRET Function for Monitoring the Gelation and Formation of Nanoparticles Based on Chitosan Copolymers

Igor D. Zlotnikov , Ivan V. Savchenko , Elena Vadimovna Kudryashova *

Posted Date: 22 June 2023

doi: 10.20944/preprints202306.1629.v1

Keywords: FRET; chitosan; nanoparticles; gelation; fluorescent probe; ovalbumin

Article

Fluorescent probes with FRET function for monitoring the gelation and formation of nanoparticles based on chitosan copolymers

Igor D. Zlotnikov, Ivan V. Savchenko [1] and Elena V. Kudryashova *

Faculty of Chemistry, Lomonosov Moscow State University, Leninskie Gory, 1/3,
119991 Moscow, Russia; zlotnikovid@my.msu.ru (I.D.Z.); ivan.savchenko@chemistry.msu.ru (I.V.S.)
* Correspondence: helenakoudriachova@yandex.ru

Abstract: Chitosan and its derivatives as a biocompatible, biodegradable polymer that has been well-established in biotechnology and medicine as the nanogels and nanofilms forming material, has a number of practical applications in the field of the supply of medicines, food colloids, agrotechnology, as well. In this paper, the focus of attention is the study of physico-chemical principles of the gels and nano-particles formation using fluorescence spectroscopy methods. We have obtained chitosan (Chit5) and pegylated chitosan (Chit5-PEG) particles with an average size of 170 or 400 nm, respectively by counterflow extrusion method. The paper presents three based fluorescent probes sensitive to the formation of chitosan particles: congo red, malachite green as well as covalently attached pyrene-label. Dyes fluoresce about an order of magnitude brighter in the composition of chitosan nanogel particles. With these fluorescence probes, the pH- and temperature-dependent behavior of polymers was studied, and the influence of the genipin-based crosslinking agent on the gel formation parameters, such as kinetics and concentration dependence of the nanoparticles formation accompanied by sharply increases in the fluorescence intensity of dyes was evaluated. A sensitive approach for tracking gelation and including of small drug molecules and protein by FRET using a pyrene-tryptophan donor-acceptor pair is proposed using tryptophan or ovalbumin as fluorophores-donors. Upon nanogel formation FRET effect is observed manifested in sharp increase if the fluorescence intensity of the pyrene (acceptor). Thus, the application of the fluorescent probes with FRET function for monitoring the gelation and nanoparticles formation as well as drug encapsulation in chitosan-based parts, which have broad prospects in biomedical practice and food industry.

Keywords: FRET; chitosan; nanoparticles; gelation; fluorescent probe; ovalbumin

1. Introduction

Chitosan (Chit) is a linear copolymer of D-glucosamine and N-acetyl-D-glucosamine bonded together by a β(1-4) bond, usually obtained from natural chitin polysaccharide by partial or complete deacetylation. Due to its properties, including cellular and tissue biocompatibility, as well as biodegradability, chitosan has a wide range of applications and is now being implemented in many areas [1]: environmental protection, medicine, food production, drug production, etc. This polymer is a promising structural material in medicine because of its antimicrobial [2], antioxidant and regenerative activity [3], as well as the possibility of effective encapsulation of drugs, proteins [4], nucleic acids [5], eukaryotic cells [6], bacteria [7] and viruses [8]. Chitosan is also widely used as a feed additive, due to its proven ability to accelerate weight gain, strengthen the immune system and reduce cholesterol levels in domesticated animals [9]. Of great importance in this regard is the improvement of the quality of fish feed [10], as well as the improvement of their habitat due to the effectiveness of chitosan as an adsorbent [11].

One of the features of chitosan is the ability to form nano- and microgels, the properties of which can be changed in a wide range due to chemical modification of the functional groups of the polymer, its crosslinking with other macromolecules, as well as non-covalent interaction with proteins and DNA [12,13]. Specific methods for obtaining chitosan nanoparticles of various shapes and molecular

 doi:10.20944/preprints202306.1629.v1

structure have been actively developed since their first production and include ionotropic gelation methods [14], microemulsions [15], reverse micellar method [16], emulsification by solvent diffusion [17], electrospinning [18].

It has been shown that chitosan is able to form gels in the presence of crosslinking agents, among which succinic anhydride [19,19–22], glutaraldehyde [23,24] and genipin are most often used, which covalently bind to several chitosan polymer molecules and act as bridges [25,26]. Genipin is an aglycone derived from an iridoid glycoside from the fruits of jasmine gardenia, 10,000 times less toxic than glutaraldehyde. Moreover, genipin has anti-inflammatory, anti-angiogenic properties, is used for liver disorders, stimulates the release of insulin. Cross-linking with other macromolecules and polymers is often used to change the physico-chemical parameters of gels - mechanical strength, sensitivity to medium acidity, biodegradability, etc. Crosslinking of polymer chains with simultaneous capture of the fluorophore inside the polymer tangle (chemical gelation) significantly affects the properties of the probe, more strongly than physical gelation.

Gelation can also occur in the presence of coordinating heavy metal ions interacting between polymer molecules. The formation of gels and nanoparticles in such conditions depends very much on the concentration of the crosslinking agent, the acidity of the medium and temperature, which can also be used in the development of methods for obtaining particles of a certain size and density [27].

FRET (Förster resonance energy transfer) can be considered as a promising method of analysis of nanoparticles formation, which consists in the interaction of two fluorophore molecules resulting in a change in the wavelength of radiation due to intermediate energy transfer to the acceptor after the donor is excited [28]. Due to the strong dependence of the efficiency of such transfer on the chemical environment of fluorophore molecules and the distance between them, FRET is widely used in studying the structure of chitosan itself [29], materials based on it [30] as well as nanoparticles [31,32]. In addition to determining the physico-chemical parameters of labeled particles based on chitosan, the FRET phenomenon is also used to modulate their fluorescence spectrum [33,34]. For FRET phenomenon tryptophan (also in protein) and pyrene, respectively, can be effectively used [35,36]. In the present work, gelation process was studied using FRET between pyrene-labeled Chit5 and Chit5-PEG as acceptors and Trp or ovalbumin Trp as donors.

One of the most important aspects of chitosan is the possibility of modifying its nanoparticles with fluorophores, which is actively used in bio-imaging technology used both in clinical practice and in fundamental research [37–39]. In this case, the fluorophore molecule can be adsorbed by the polymer [40] or bind to it covalently [41]. In the present work pyrene as covalent probe, congo red and malachite green as non-covalent fluorophores as fluorophores sensitive to local microenvironment and folding of polymer chains.

Physicochemical parameters of polymers prone to gelation, such as solubility, sensitivity to acidity of the medium, fluorescence intensity and position of maxima, optical absorption spectrum, kinetic and thermodynamic stability, strongly depend on the conditions of preparation and structural features of the polymer [42,43]. When polymeric nano(micro)particles are formed, the intensity of dye fluorescence may ignite due to changes in the microenvironment or fluorescence quenching during the formation of large particles and a significant increase in the viscosity of the solution.

Fluorescent probes (including those with the FRET option) can be effectively used to study the formation of particles from modified chitosans, for example, pegylated chitosans capable of forming thermogels [44]. In this regard, polyethylene glycol (PEG) is often used, the molecules of which can be bound to amino groups in the chitosan molecule and thus obtain a polymer (Chit-PEG) with increased solubility in water and greater stability [45,46]. Modified chitosan nanoparticles find extremely important use in medicine due to their ability to include nutrients, drugs, peptides, nucleic acids, viruses, etc. In connection with these applications of chitosan, it is expected to increase the effectiveness of the treatment of malignant tumors and reduce the toxicological effect of the drug on the body due to the controlled release of the drug in the pathogenic region [12]. It has been shown that due to the presence of reactive functional groups in chitosan and, as a consequence, the wide possibilities of conjugating it with numerous proteins, lipids and with specific molecules capable of binding to pathogenic cells of the body, it is possible to develop methods of targeted effective therapy

 doi:10.20944/preprints202306.1629.v1

of oncological diseases [47,48]. Varying the particle sizes and their physico-chemical properties also makes it possible to reduce the side effects of drugs, their effective dose and at the same time increase the time of excretion from the body [24].

When studying the organization of chitosan-based nanoparticles, infrared and optical absorption spectroscopy are often resorted to, which makes it possible to prove the binding of the crosslinking agent with chitosan [49,50]. In order to determine the stability of the colloidal system of nanoparticles and their size, electrokinetic measurements and measurement of static light scattering are used, respectively [51].

Thus, this work is devoted to the development of the approach based on the fluorescent methods (with the FRET option) to study the physicochemical aspects of particle formation depending on pH, temperature, and the presence of a crosslinking agent, which is promising for creating optimal biomedical gels, ointments, and dosage formulations. The inclusion of ovalbumin in polymer particles is interesting in aspects of potential application in the biomedicine (including vaccine formulations), food industry for the creation of foams and emulsions, gels, mousses, in cosmetology.

2. Materials and Methods

2.1. Reagents

Chitosan oligosaccharide lactate 5 kDa (Chit5), activated PEG 5 kDa (N-succinimidyl ester of mono-methoxy poly(ethylene glycol)), ovalbumin, tryptophan (Trp), 1M 2,4,6-trinitrobenzenesulfonic acid (TNBS) were purchased from Sigma Aldrich (St. Louis, MI, USA). 1-pyrenebutanoic acid succinimidyl ester was bought from Invitrogen (Molecular Probes, Eugene, OR, USA). Congo red and malachite green were kindly presented by Sergey Krylov (Senior Researcher, Zelinsky Institute of Organic Chemistry, RAS).

2.2. Chitosan PEGylation and pyrene-modification

Chit5 was pegylated according to previously reported technique [44] with small modification. Chit5-PEG5 copolymer was obtained by reaction between Chit5 aminogroups and activated carboxylic group of PEG. The samples of the components in the same mass ratio were mixed and dissolved in PBS, the mixture was heated to 60 °C and incubated for 4 hours. Copolymer was freeze-dried at –70 °C (Edwards 5, BOC Edwards, UK).

Chit5 and Chit5-PEG in concentrations of 1 mg/mL (to achieve optimal modification rate) were pyrene-modified by amino group reaction with activated pyrene (1-pyrenebutanoic acid succinimidyl ester) in PBS (pH 7.4) for 72 h at 40 °C (Scheme is presented on Figure 1b, kinetic curves are presented on Figure 2d). Molar ratio Chit5:pyrene = 2:1, Chit5-PEG:pyrene = 2.5:1

The degree of Chit5 modification be PEG or pyrene was determined using A420 values for amino group adducts with 2,4,6-trinitrobenzenesulfonic acid (TNBS) in 0.02 M sodium borate buffer (pH 9.2).

2.3. Nanoparticles obtaining and characterization

Chit5 and Chit5-PEG nanoparticles was obtained using extrusion (200 or 400 nm membrane, Avanti Polar Lipids) after 1 h incubation of samples (0.01-1 mg/L) at 40 °C. The initiation of gelation was performed by placing a solution with an alkaline medium (pH 8-10), ovalbumin or alginic acid as the counterions in a syringe receiver.

Particles hydrodynamic diameter sizes and ζ-potentials were measured using Zetasizer Nano S «Malvern» (Malvern, UK) (4 mW He–Ne laser, 633 nm, scattering angle 173°) in 0.01 M PBS (pH 7.4). Dynamic Light Scattering data were analyzed using «Zetasizer Software» (v. 8.02).

2.4. Fluorescence approach to study of nanoparticles and gel formation

Fluorescence emission spectra were recorded on a Varian Cary Eclipse fluorescence spectrometer (Agilent Technologies, USA). λ_{exci}(pyrene) = 330 nm.

 doi:10.20944/preprints202306.1629.v1

2.5. FTIR Spectroscopy

FTIR spectra of samples were recorded using a Bruker Tensor27 spectrometer equipped with a liquid nitrogen-cooled MCT (mercury cadmium telluride) detector, as described earlier [52–55].

3. Results and Discussion

The research is aimed at developing the sensitive approach based on the fluorescent methods to monitor the formation of chitosan-based particles and gels. The main steps in the work to understand the physico-chemical principles of gelation are as follows:
i) Synthesis of polymers and characterization of their molecular composition using FTIR spectroscopy before gelation, as well as obtaining particles by various methods, including extrusion with counterion coacervation; ii) Comparison of the properties of volume-phase macrogel with nanoparticles using fluorescent probes. Optimization of gelation conditions with subsequent particle formation under certain conditions; iii) Studying of the particle's formation depending on temperature, pH, polymer concentration, the presence of a crosslinking agent using non-covalent fluorescent probes (malachite green and congo red) determination of gelation conditions and nanoparticles formation; iiii) Application of covalently attached to chitosan chain pyrene probe to monitor nanoparticles formation as well as encapsulation of the cargo : inclusion of a small molecule (tryptophan as model drug molecule) and a protein (ovalbumin) into pyrene-labeled chitosan particles as a simulation of loading of drugs into polymer carriers and demonstration of a new technique for tracking inclusion using FRET

3.1. Polymers and particles characterization

Figure 1 shows the FTIR spectra of Chit5 and Chit5-PEG in D_2O, which makes it possible to monitor the oscillations of N–H and O–H bonds in solution. FTIR spectroscopy provides valuable data on the microenvironment and the state of functional groups. When modifying chitosan amino groups with PEG, an increase in the peak corresponding to the oscillations of N-H bonds (3400 cm^{-1}) is observed, but only using D_2O as a solvent, since in H_2O these oscillations are "banned". The Chit5-PEG conjugate exhibits an intense absorption loss of C-H bond oscillations (weak intensity in simple chitosan) of 2850-2970 cm^{-1}, and the intensity of amide 1 and amide 2 peaks corresponding to valence oscillations C=O and deformation oscillations N-H increases. The most striking fact confirming the presence of both components in the Chit5-PEG conjugate is the changes in the shape of the peak corresponding to the oscillations of the C-O bonds (1100 cm^{-1}), since the functional groups of both chitosan and PEG contribute.

Preprints (www.preprints.org) | NOT PEER-REVIEWED | Posted: 22 June 2023 doi:10.20944/preprints202306.1629.v1

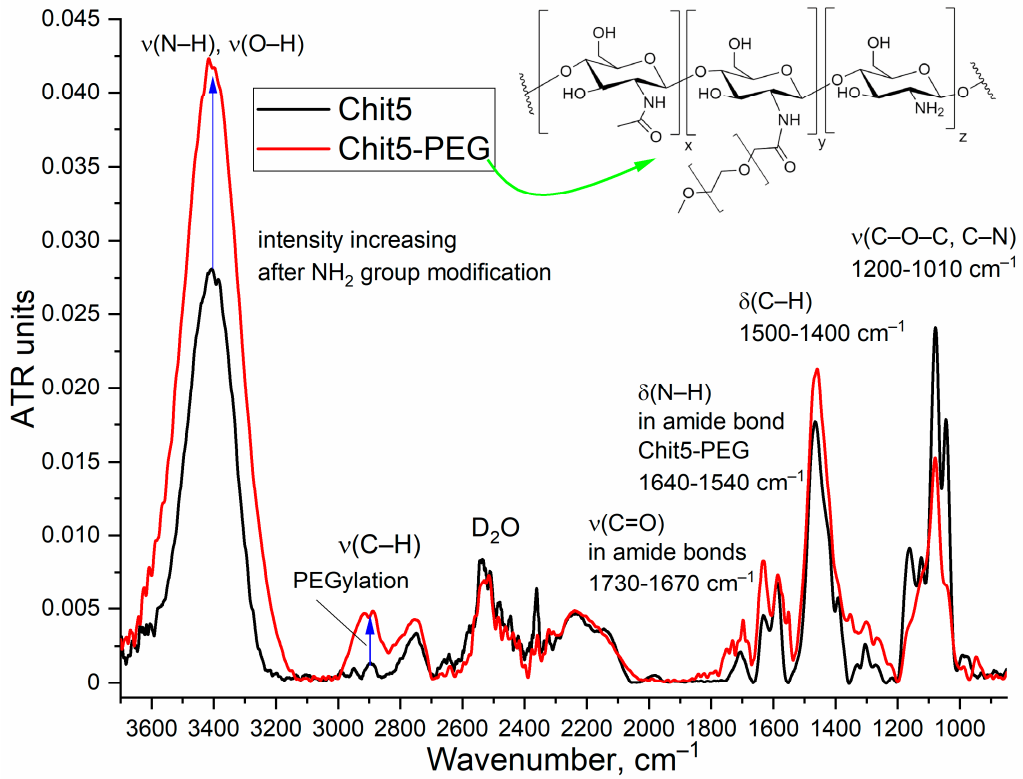

Figure 1. FTIR spectra of Chit5 and Chit5-PEG in D_2O. T = 22 °C.

Important parameters characterizing the stability of the colloidal system of particles and their structure are the zeta potential and the radius of the particles. The zeta potential is the potential difference between the dispersion medium and the stationary liquid layer surrounding the particle. This value shows the stability of this colloidal system and the tendency of particles to coagulate [56]. The radius of the particles also affects their properties and determines the scope of their applications.

An interesting aspect is the comparison of volume phase gel and nanogel, as well as the variation of gel-initiating conditions (pH or counterion). During gel extrusion, particles were formed due to a sharp change in pH from 6 to 10 or due to interaction with counterion (alginic acid): a counterflow of Chit5 or Chit5-PEG solutions meets with an anti-solvent in an extruder camera with the formation of poly- and interpolyelectrolyte complexes. The method of particles preparation can be reflected on their properties.

Table 1 presents data on the hydrodynamic size and zeta potential of particles formed by Chit5 and Chit5-PEG gelation compacted with the situation where alginic acid used as counterion. Chit5 in a dilute solution at pH 7.4 forms bulky aggregates, because the charge of amino groups is lost in a neutral medium, and polymer chains stick together (almost zero zeta potential). At the same time, PEGylated Chit5 has increased solubility and forms 450 nm nanoparticles. After extrusion, homogeneous, neat particles with hydrodynamic radius of 170 nm (Chit5) and 400 nm (Chit5-PEG) are obtained. In the case of PEG-chitosan, the hydrodynamic volume is greater due to PEG hydration shell [57].

Alginic acid, negatively charged polysaccharide, forms electrostatic complexes with chitosan during extrusion, the counterflow of chitosan particles undergoes coacervation due to compensation of charges of counterions of alginic acid polyanions. Chit5-(alginic acid) particles have a larger size than Chit5 particles. On the contrary, Chit5-PEG-(alginic acid) particles are compacted by polyanion as crosslinking agent (Table 1).

The recharge of chitosan particles upon coacervation with alginic acid is observed due to formation of polyelectrolyte complexes (Table 1). This recharge is more pronounced in Chit5 than in Chit5-PEG (in which chitosan chains are partially shielded), which is reflected in the values of zeta potentials –15 mV vs –5.5 mV.

 doi:10.20944/preprints202306.1629.v1

Table 1. Physico-chemical parameters of particles formed by Chit5 and Chit5-PEG compacted with alginic acid (30-50 kDa, 2-fold molar excess). Concentration of polymers 0.1 mg/mL. PBS (0.01 M, pH 7.4). Extrusion was performed in borate buffer with pH 10, or alginic acid (pH 7.4).

Polymer	Sample	Hydrodynamic diameter of particles, nm	ζ-potential, mV
Chit5 (5 kDa, 90% degree of deacetylation)	native	> 1μm	0.7±0.3
	400 nm extrusion in pH 10	170±40	–1.9±0.8
	400 nm extrusion in solution with alginic acid	260±40	–15±2
Chit5-PEG (1/1 w/w, 10 kDa)*	native	450±70	3.5±0.9
	400 nm extrusion in pH 10	400±30	–0.3±0.2
	400 nm extrusion in solution with alginic acid	190±10	–5.5±1.9

*determined by FTIR (Figure 1) and by the number of amino groups in Chit5 by TNBS-titration before and after modification.

3.2. Grafting of polymers with pyrene

3.2.1. FTIR spectroscopy

For studying gel or particle formation using fluorescent approach was applied with using pyrene probe covalently attached to chitosan chain (Figure 2a). The introduction of a pyrene label into polymers significantly affects the FTIR spectra (Figure 2b): characteristic peaks of C-C(aromatic) oscillations appear (1500-1600 cm^{-1}) and the peak intensity of oscillations of the C=O and N-H in amide bond increases. On average, 0.5 and 0.4 pyrene molecules per Chit5 and Chit5-PEG polymer molecule, respectively (based on UV spectroscopy data on pyrene absorption (Figure 2c) and data on the number of amino groups by TNBS-titration).

3.2.2. UV and fluorescence spectroscopy

Covalent crosslinking of activated pyrene with Chit5 and Chit5-PEG leads to a change in the microenvironment of the fluorophore, which is reflected in the shift of absorption maxima from 354 to 342-343 nm and from 336 to 327-328 nm (Figure 2c) this spectral change itself can serve as an analytically significant signal (modification or gelation). In the literature, data on the non-covalent pyrene label are described [58–60], however, show less sensitivity and informativeness in comparison with covalent [36,53,61,62]. In the covalent conjugate pyrene fluoresces much brighter than the free fluorophore (Figure 2d). The kinetic curves of pyrene grafting to polymers is presented in Figure 2d, where two stages can be distinguished: 1) 0-2 hours – mainly covalent crosslinking of pyrene with chitosan, 2) 2-72 hours – mainly folding of the polymer into a globule due to the use of medium-gel-forming concentrations.

Preprints (www.preprints.org) | NOT PEER-REVIEWED | Posted: 22 June 2023 doi:10.20944/preprints202306.1629.v1

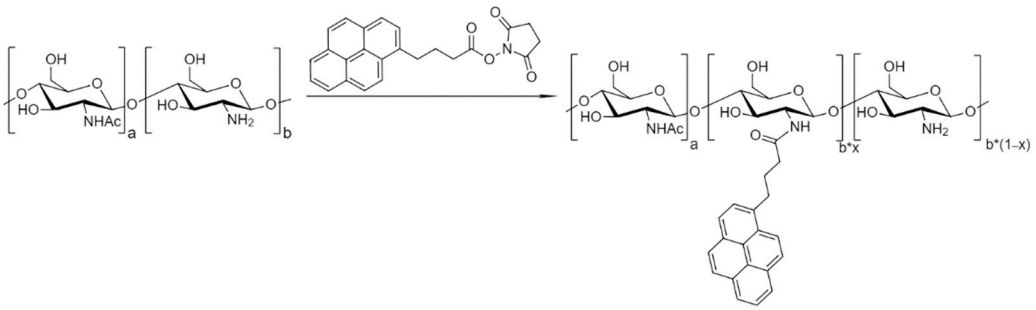

(a)

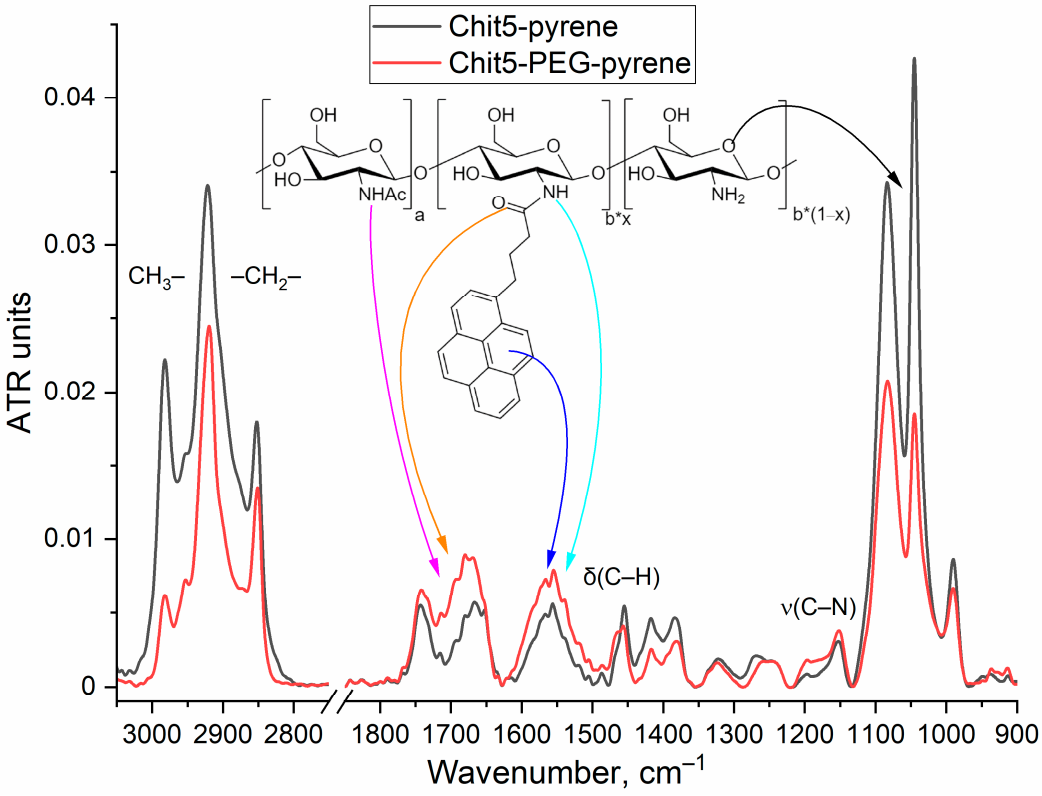

(b)

Preprints (www.preprints.org) | NOT PEER-REVIEWED | Posted: 22 June 2023 doi:10.20944/preprints202306.1629.v1

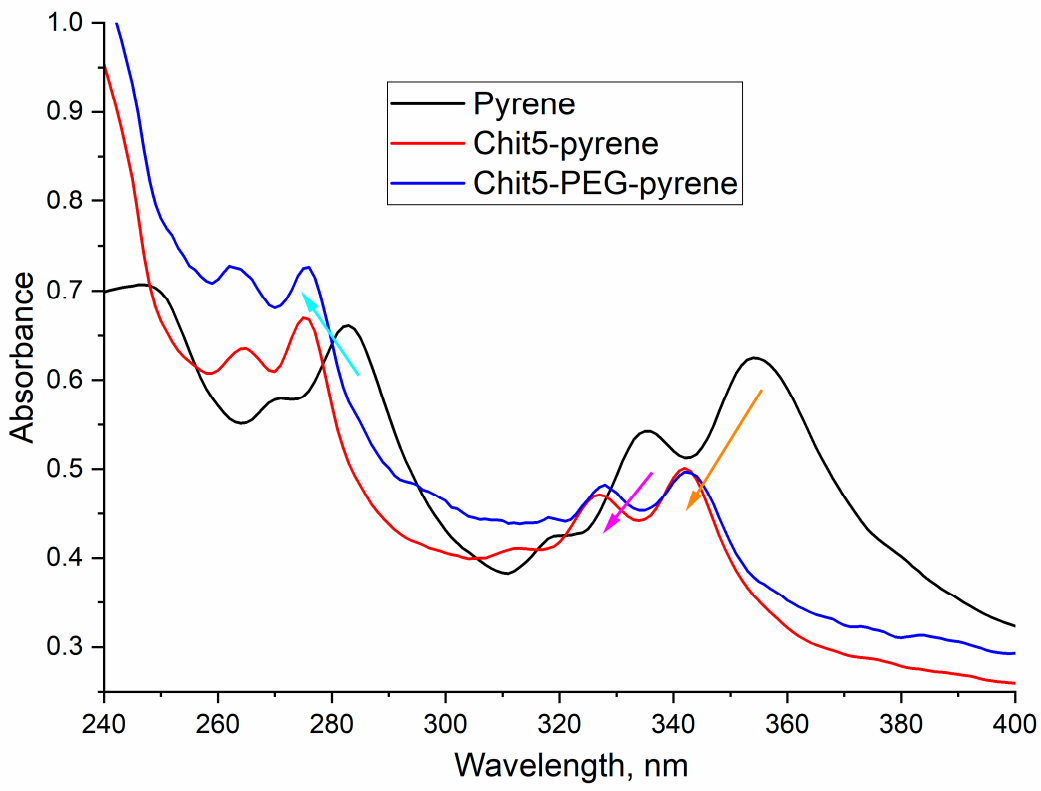

(c)

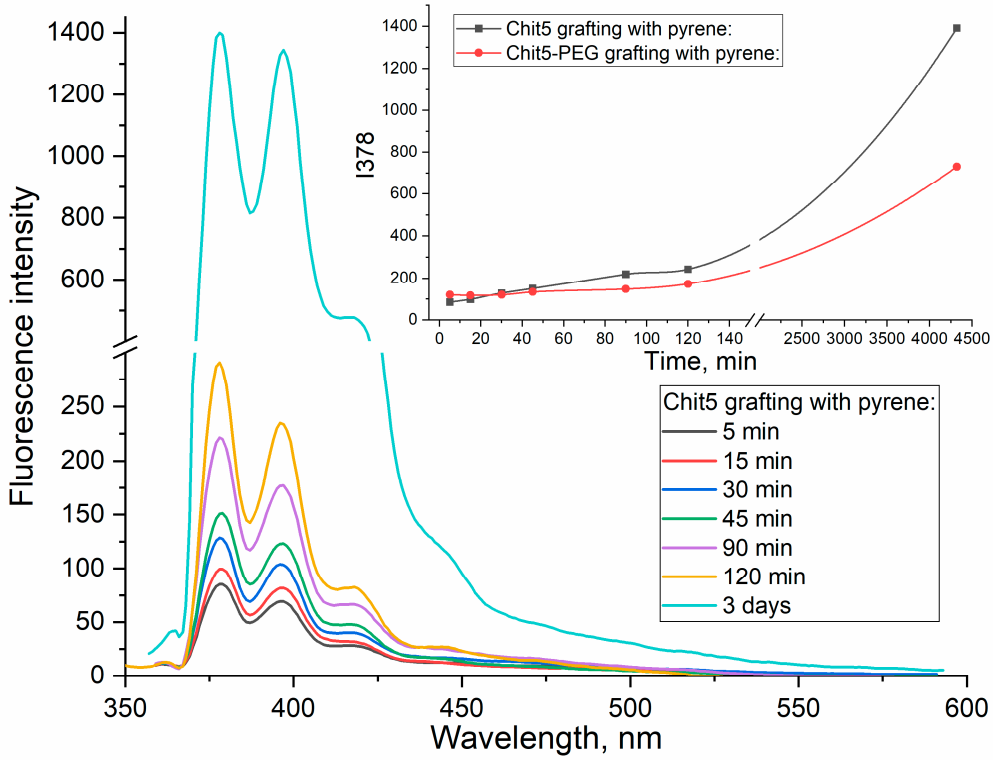

(d)

Figure 2. (a) Scheme of synthesis of pyrene-grafted Chit5 (for Chit5-PEG the reaction is similar). (b) FTIR spectra of Chit5-pyrene and Chit5-PEG-pyrene. PBS (0.01M, pH 7.4). T = 22 °C. (c) UV spectra of activated pyrene and pyrene crosslinked with Chit5, Chit5-PEG in PBS-DMSO (0.01% DMSO v/v).

Preprints (www.preprints.org) | NOT PEER-REVIEWED | Posted: 22 June 2023 doi:10.20944/preprints202306.1629.v1

(d) Fluorescence spectra of pyrene during conjugation with polymers and corresponding kinetic curves. PBS (0.01M, pH 7.4). T = 40 °C.

3.3. Gel or nanoparticles formation

3.3.1. Pyrene probe to optimize the conditions for the formation of macrogels (in volume-phase)

The formation of marogels studied in detail using fluorimetry with a pyrene probe (Figure 3). Covalent pyrene is a suitable probe for micelle formation [36,53,58–63], probably this label is also applicable for studying of gelation, since the microenvironment in chitosan becomes hydrophobic during gelation. During the formation of chitosan volume-phase gel a change in the pyrene microenvironment takes place, and fluorescence quenching is observed.

To monitor the gelation, the follows scheme of the experiment was applied: a starting solution where chitosan is soluble at pH 2.5 (all of amino groups are charged) was used and gelation was initiated by changing the pH to 3.0, 7.4 or 10.5. Chit5-PEG at pH 3.0 and 7.4 forms particles with a size of 400-500 nm. In an alkaline medium, the solubility of Chit5-PEG decreases, which leads to the formation of sol (visually, but not pieces of polymer as in the case of simple chitosan). At pH 3, the formation of particles practically does not occur for both polymers, but after initiation from pH 8-10, changes in the pyrene fluorescence are pronounced (Figure 3).

Copolymers Chit5-PEG can self-organize into polymeric micelles in aqueous solution: hydrophobic Chit5 form the core of micelles, while hydrophilic PEG chains interact with water molecules in the "PEG-corona" to ensure the solubility of the hydrogel [44,64]. As result, fluorophore molecules change the fluorescence properties dramatically when the microenvironment changes, when pyrene is incorporated into the hydrophobic core.

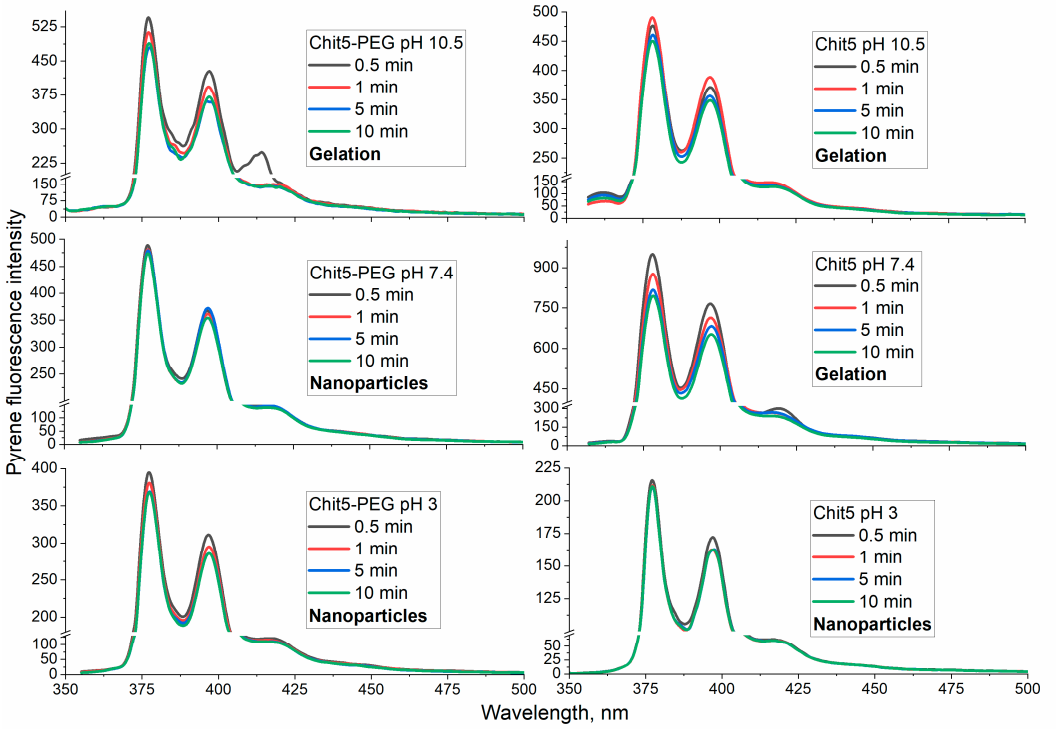

Figure 3. Fluorescence spectra of pyrene-grafted Chit5 and Chit5-PEG during gel or nanoparticles formation at different pH. $C_{polymer}$ = 1 mg/mL. Gelation was pH-induced. T = 40 °C. λ_{exci}(pyrene) = 330 nm.

3.3.2. Ignition of dye fluorescence as indicator of volume-phase macrogel formation

Congo red and malachite green were chosen by us as non-covalent fluorescent probes for monitoring the formation of chitosan particles to study the change in the fluorescence spectrum during the transition from an aqueous solution to a hydrophobic region in a polymer tangle. Figure

Preprints (www.preprints.org) | NOT PEER-REVIEWED | Posted: 22 June 2023 doi:10.20944/preprints202306.1629.v1

4 shows the emission spectra of fluorescence dyes in PBS, DMSO, as well as in the composition of polymer chitosan particles. When incorporated into the chitosan particles, there is a sharp increase in the fluorescence of both dyes by about an order of magnitude - this phenomenon can be used as a fluorescent probe for gelation.

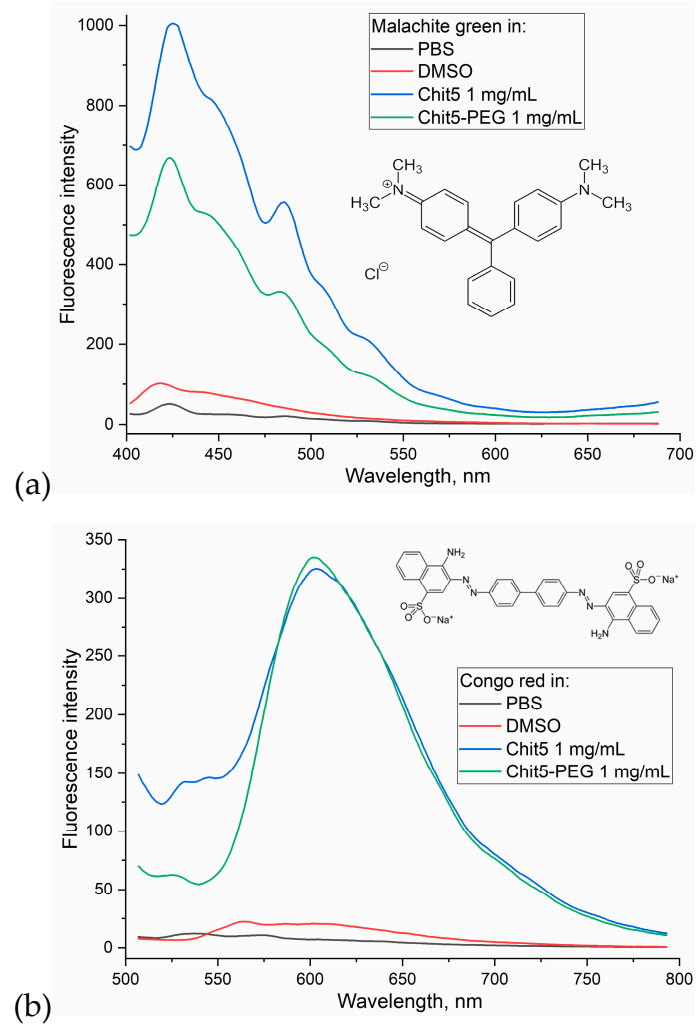

Figure 4. Fluorescence spectra of congo red and malachite green (10 μg/mL). T = 40 °C. λ_{exci}(malachite green) = 370 nm, λ_{exci}(congo red) = 480 nm.

3.3.3. pH-sensitive volume-phase gel formation

pK_a of chitosan ≅6.3-6.4, therefore, at pH below 6 chitosan is soluble, and at neutral or alkaline pH values it is prone to aggregation due to loss of charge of amino groups. For Chit5-PEG, this effect is leveled by hydrophilic PEG chains that maintain solubility in a wide pH range. Using the probe described above, the pH-dependent character of gelation kinetics was studied. Figure 5 shows the kinetic curves of the fluorescence emission of a fluorescent probe (congo red) after pH-initiated gel formation. At pH 6.2, Chit5 and Chit5-PEG form nanoparticles (a small increase in fluorescence), while the degree of inclusion of dye in pegylated chitosan is 2.5 times higher than in unmodified (as can be judged from the values of fluorescence emission). At a physiological pH value of 7.4, chitosan aggregates with the formation of microparticles, Chit5-PEG forms nanoparticles (the upward curve) and the capture of congo red is observed in both cases (Figure 5, Table 1). Chit5-PEG almost instantly formed nano- and microparticles in pH 8.4, and at pH 10.5 precipitates large aggregates (the downward curve), and the capture of the dye from the solution is observed. Chit5 aggregates rapidly at pH>8 and precipitates as large polymer particles. Thus, pegylated chitosan can be used in medicine, since it forms stable particles in a wide pH range.

Preprints (www.preprints.org) | NOT PEER-REVIEWED | Posted: 22 June 2023 doi:10.20944/preprints202306.1629.v1

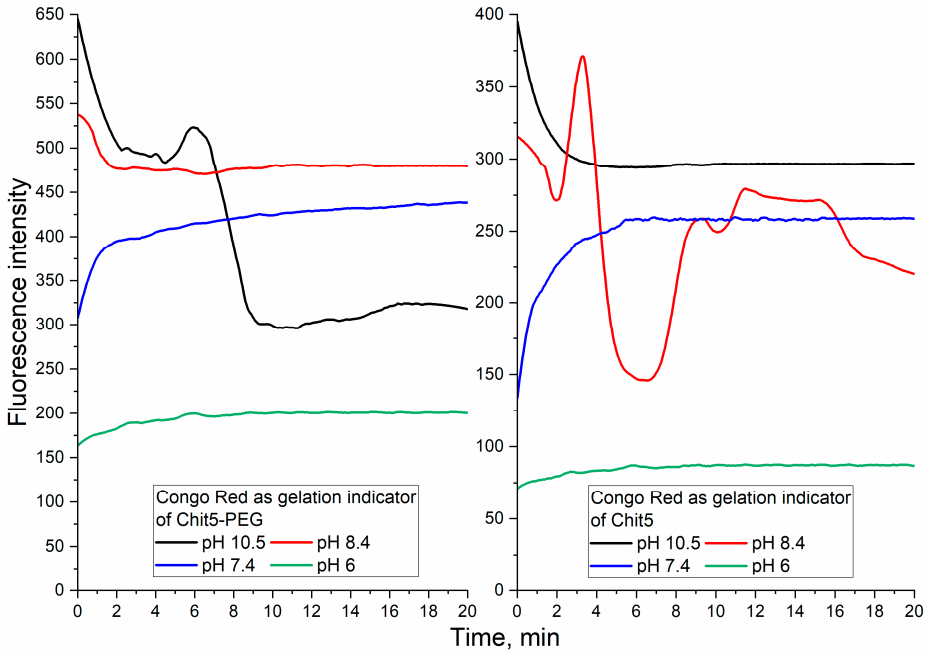

Figure 5. Kinetic curves of congo red (10 μg/mL) fluorescence emission during particles and gel formation by Chit5 and Chit5-PEG. T = 40 °C. λ_{exci}(congo red) = 480 nm. The curves were normalized to the values of free dye emission at a given pH.

3.3.4. Concentration dependences of gelation

Fluorescence polarization characterizes the rotation of plane-polarized light, which is chaotic for small fluorophores and has specific values for fluorophores associated with large molecules (proteins, polymers, DNA, etc.). Figure 6a shows the polarization spectra of congo red fluorescence depending on the concentration of the added polymer. It is expected that with an increase in the concentration of the polymer, the gel-forming ability increases. It is necessary to find out the critical concentration of the formation particles and how this is affected by PEGylation and how gelation is reflected on fluorescent probes. Chit5 at a concentration of 1 μg/mL and above forms nano- and microparticles, which is reflected in a sharp increase in fluorescence polarization. Chit5-PEG at a concentration of 1 μg/mL forms nanoparticles (50-100 nm by DLS, polarization 0.13), above 5-10 μg/mL 400 nm particles (by DLS, polarization 0.4-0.5) are formed.

In order to study the issue of gelation in more detail, fluorescence emission spectra were recorded depending on the concentration of polymers (Figure 6b). Up to a concentration of 1 mg/ml Chit5-PEG and 0.1 mg/mL Chit5, the fluorescence emission of the probe is ignited, which indicates an increase in the particle size and the degree of inclusion of the dye, accompanied by a shift of the maximum to the long-wavelength region by 10-20 nm (Figure 6bc). With a higher concentration of polymers, fluorescence quenching is observed due to the formation of large aggregates giving a reflection of 500-550 nm, which is consistent with the fluorescence polarization data.

Preprints (www.preprints.org) | NOT PEER-REVIEWED | Posted: 22 June 2023 doi:10.20944/preprints202306.1629.v1

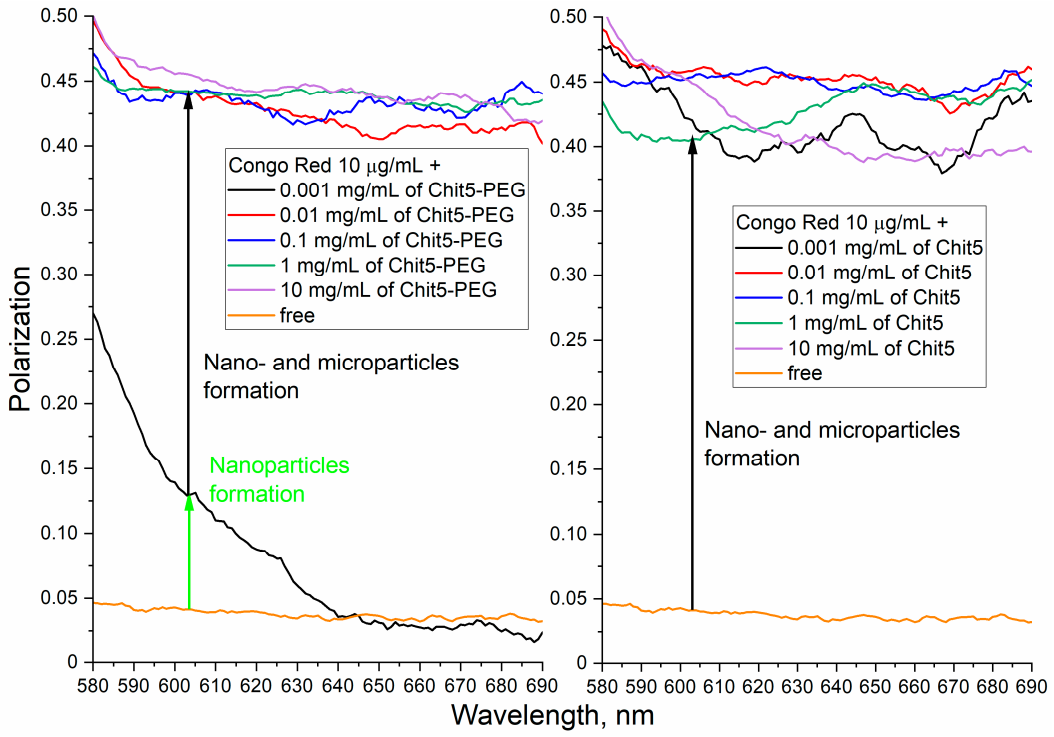

(a)

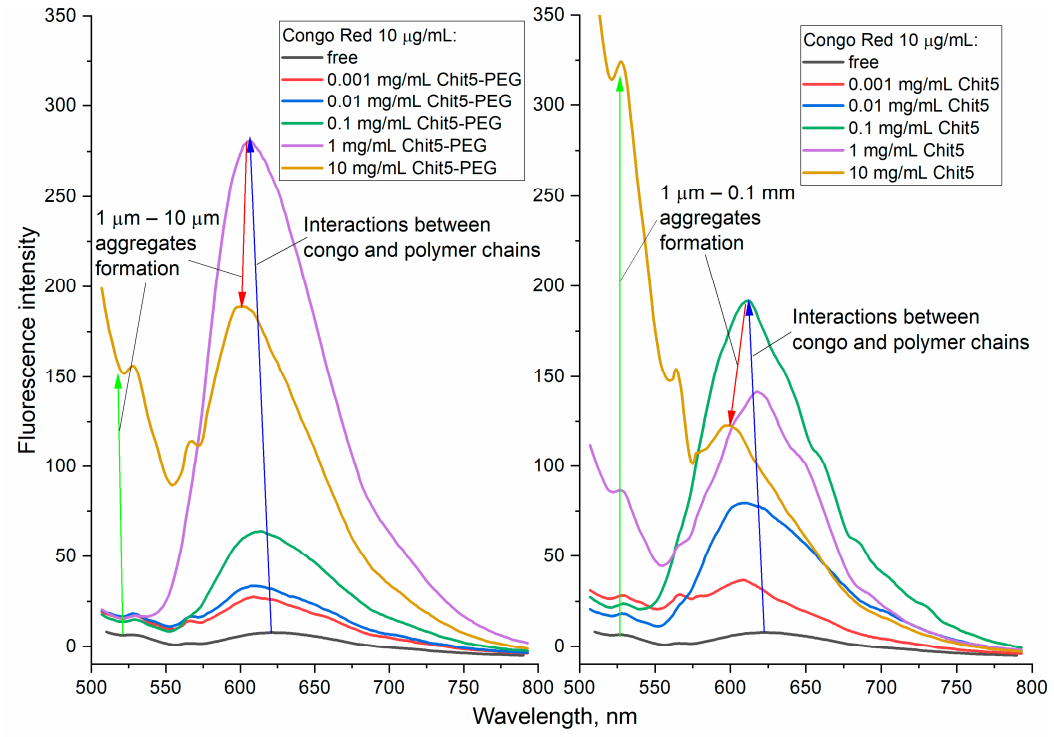

(b)

Preprints (www.preprints.org) | NOT PEER-REVIEWED | Posted: 22 June 2023 doi:10.20944/preprints202306.1629.v1

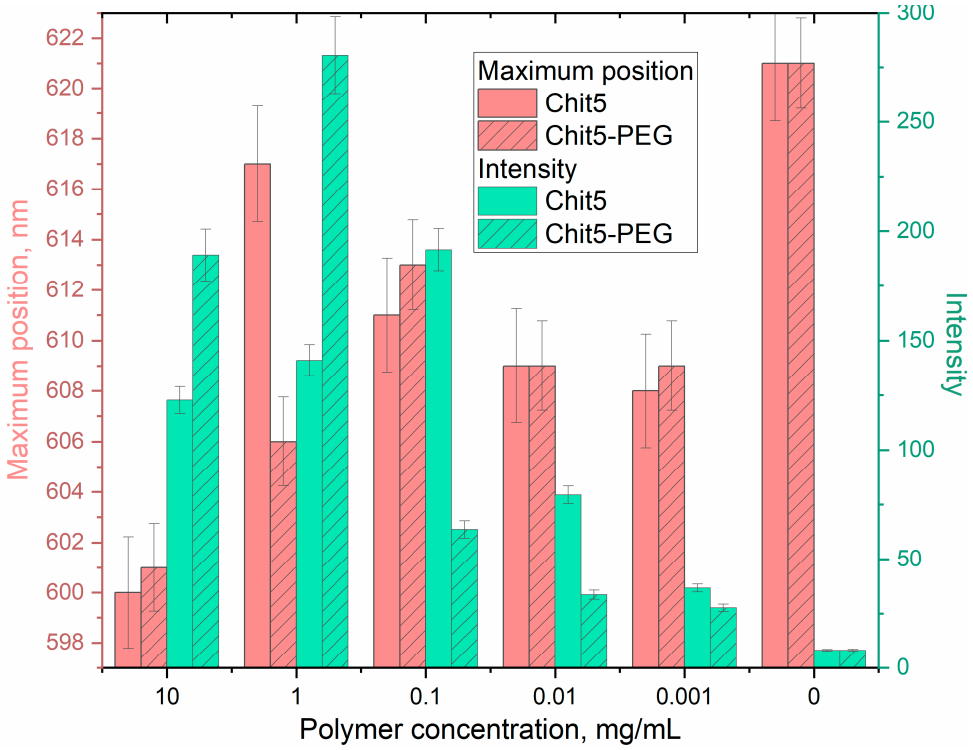

(c)

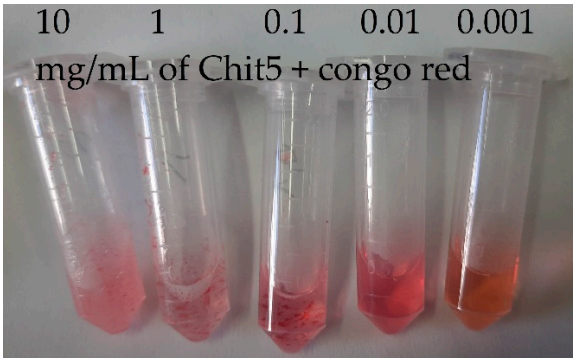

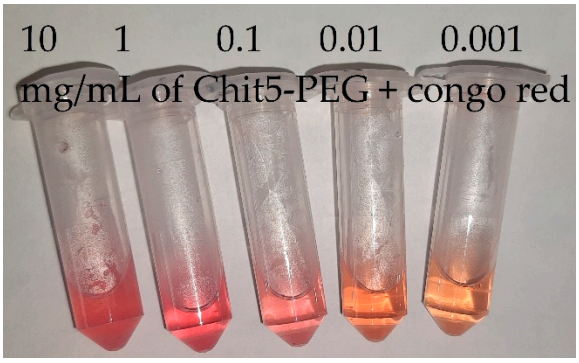

(d) (e)

Figure 6. Fluorescence approach to study the concentration dependence of gelation: (a) Fluorescence polarization spectra, (b) emission spectra, (c) corresponding dependences of maxima positions and intensity. Congo red (10 μg/mL) was used as probe. PBS (pH 7.4). T = 40 °C. λ_{exci}(congo red) = 480 nm. (d)-(e) Photos of samples 30 min of incubation. Chit5 forms colored polymer pieces, and Chit5-PEG forms a stable colloidal system.

3.3.5. Temperature dependences of gelation

The application of a fluorescent probe to monitor gelation provides valuable information about the flexibility of the polymer chain or hydrophobic sites formation, for example, when using a covalent pyrene label [65]. Previously, we described a technique for tracking gelation or micelles formation using rhodamine 6G, but its sensitivity is low and can be improved by using congo red and malachite green [44,66]. Gelation is accompanied by an increase in the viscosity of the solution, an increase in hydrophobicity due to the aggregation of polymer chains, which can potentially affect the fluorescence of the dye [67,68].

Due to strengthening the hydrophobic interactions of chitosan chains at high temperature the gelation is observed. However, in the case of unmodified chitosan, large aggregates are formed. Contrariwise, pegylated chitosan forms volume-phase gel.

Preprints (www.preprints.org) | NOT PEER-REVIEWED | Posted: 22 June 2023 doi:10.20944/preprints202306.1629.v1

Figure 7 shows thermograms of Chit5 and Chit5-PEG gelation studied using congo red probe. The direct and reverse processes of phase transitions were studied, since they are important for understanding the reversibility and stability of the formed particles. When the temperature increases, the fluorescence quenches due to both the temperature factor and gelation. For Chit5, there is almost a coincidence of the forward and reverse path (the process of dye inclusion and particle formation is fast and reversible). For pegylated chitosan, the curve of the reverse process lies significantly below the curve of the direct process and does not come to the starting point, which means that the destruction of the gel from Chit5-PEG is practically not observed. So, once formed, the gel will be stable even at lower temperatures.

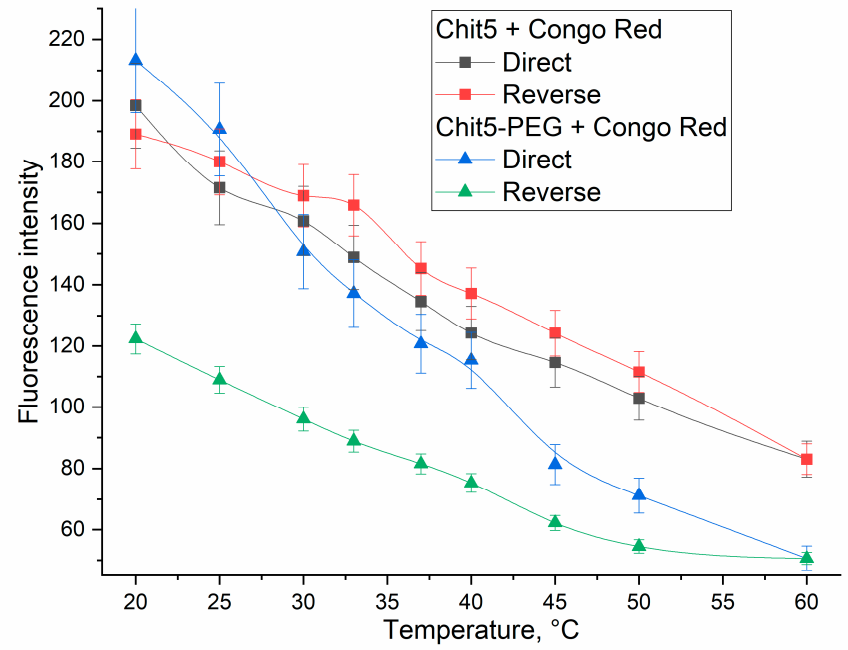

Figure 7. Thermo-curves of congo red (10 μg/mL) fluorescence emission during particles and gel formation by Chit5 and Chit5-PEG. λ_{exci}(congo red) = 480 nm. PBS (pH 7.4).

3.3.6. Genipin cross-linked polymers

Chemical gelation, in contrast to the physical one (described above), can have a number of interesting new properties. Chemical crosslinking of polymer chains can be performed with bifunctional crosslinking agents (diisothiocyanates [69,70], dialdehydes [23,24], activated derivatives [71–76]), however, the issue of safety and biocompatibility is important for use in medical practice. Genipin is 10,000 times less toxic than glutaraldehyde, and has been successfully used in a number of articles for crosslinking chitosan [21,25,26,77].

When crosslinking polymer chains with genipin, the microenvironment of dyes changes dramatically, but at the same time its position is quite clearly fixed in the tangle of polymer (Figure 8). The intensity of the fluorescence of the probes increases and the shift to the wavelength region of the emission maximum due to an increase in the hydrophobicity of the microenvironment increases. Congo red reacts most vividly to gelation, as in the case of physical gelation. Chemical gelation causes drastic changes in the spectra of fluorescent probes. In this case, crosslinking of pegylated chitosan leads to the formation of a blue solution of particles, and insoluble flakes are formed from simple chitosan.

Preprints (www.preprints.org) | NOT PEER-REVIEWED | Posted: 22 June 2023 doi:10.20944/preprints202306.1629.v1

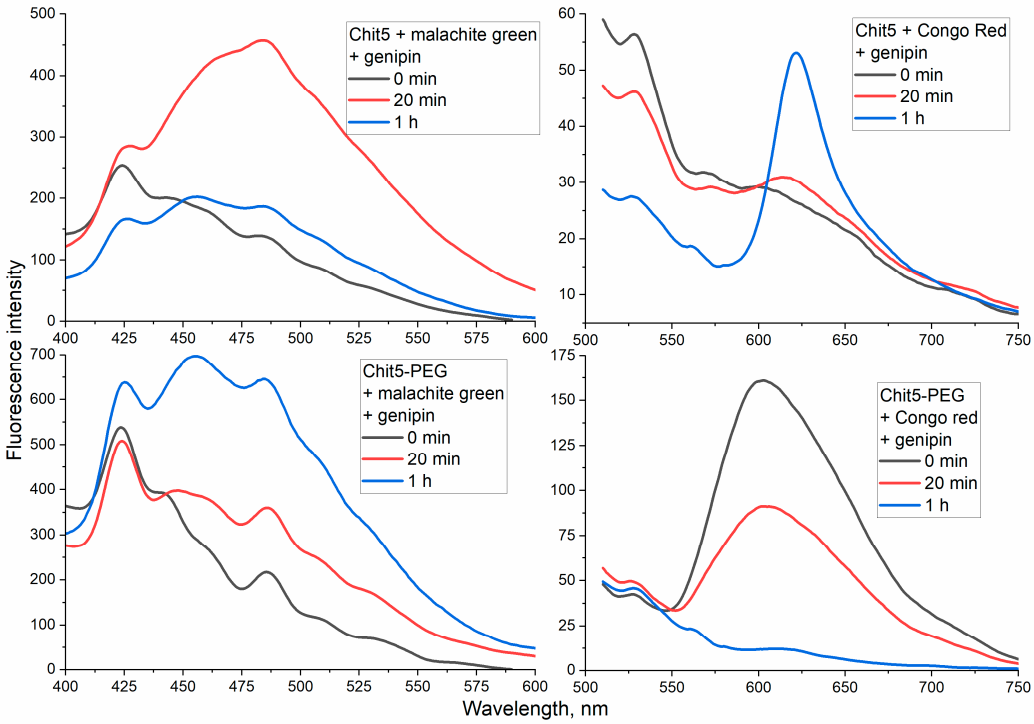

(a)

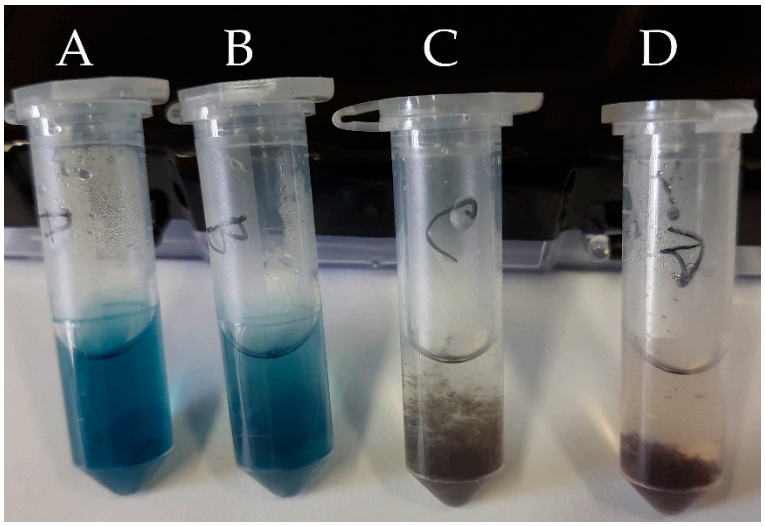

(b)

Figure 8. (a) Fluorescence spectra of congo red and malachite green (10 μg/mL) during Chit5 and Chit5-PEG chains genipin (1 mg/mL) crosslinking. T(reaction) 70 °C, T(spectra registration) 40 °C. λ_{exci}(malachite green) = 370 nm, λ_{exci}(congo red) = 480 nm. PBS (pH 7.4). (b) Photos of samples after 1 h of reaction: A – malachite green in Chit5-PEG5, B – congo red in Chit5-PEG, C - malachite green in Chit5, D - congo red in Chit5.

3.4. Förster resonance energy transfer (FRET) as a tool for study gel formation and drug molecules incapsilation

FRET is a mechanism of energy transfer between two chromophores (from donor to acceptor), which occurs without intermediate photon emission and is the result of dipole-dipole interaction between donor and acceptor [33,78–83]. FRET was effectively used to monitor gelation, since the implementation of FRET requires a spatial arrangement of fluorophores less than 10 Å, which can be realized, for example, in a hydrophobic core of micelles or in a tangle of polymer during gelation.

Preprints (www.preprints.org) | NOT PEER-REVIEWED | Posted: 22 June 2023 doi:10.20944/preprints202306.1629.v1

3.4.1. Tryptophan as a model small (aromatic) drug molecule encapsulation with FRET options

Vloume-phase Macrogels formation

We found that upon chitosan-copolymer gel formation pronounced FRET effect in pyrene-tryptophan donor-acceptor pare is observed. Figure 9a shows the fluorescence spectra of volume phase macrogel of Chit5-pyrene in the presence of tryptophan (Trp). There is a quenching of Trp fluorescence (355 nm) compared to the values observed in the absence of pyrene. There is an increase in the proportion of the short-wave pyrene component at 396 nm and a decrease in the intensity of the long-wave pyrene component (418 nm) (Figure 9a) with an increase in the concentration of Trp due to FRET.

FRET occurs when fluorophores converge, so this phenomenon should be expected during gelation this process intensified with an increase in the polymers concentration. Figure 9b shows the fluorescence spectra of pyrene-labeled polymers with added Trp at a variable polymer concentration. With an increase in the polymer concentration in the case of Chit5, pyrene fluorescence quenching is observed, and in the case of pegylated chitosan, first an increase and then a decrease in fluorescence due to the inclusion of dyes in the gel. During gelation, FRET increases, which is reflected in an increase in pyrene fluorescence while quenching tryptophan. In the absence of the polymer, FRET practically does not occur (Figure 9b, purple curve), and Trp fluorescence is mainly observed. In the presence of a high concentration of the polymer, FRET practically occurs (Figure 9b, green curve), and pyrene fluorescence is mainly observed, the spectrum is shifted to the long-wavelength region, a wide “tail” fluorescence signal is observed.

Nanogels

Figure 9c shows the fluorescence spectra of particles formed using extrusion methos by Chit5 and Chit5-PEG containing pyrene, tryptophan or mixture. After particle formation (by extrusion), due to pH initiated coacervation several times higher fluorescence observed compared to original pyrene-Chit5 and Chit5-PEG. But in the case of alginic acid used as counterion the quenching of the fluorescence was observed. FRET is intensified significantly after formation of pegylated chitosan particles by extrusion, while for non-modified chitosan the spectral differences were smaller.

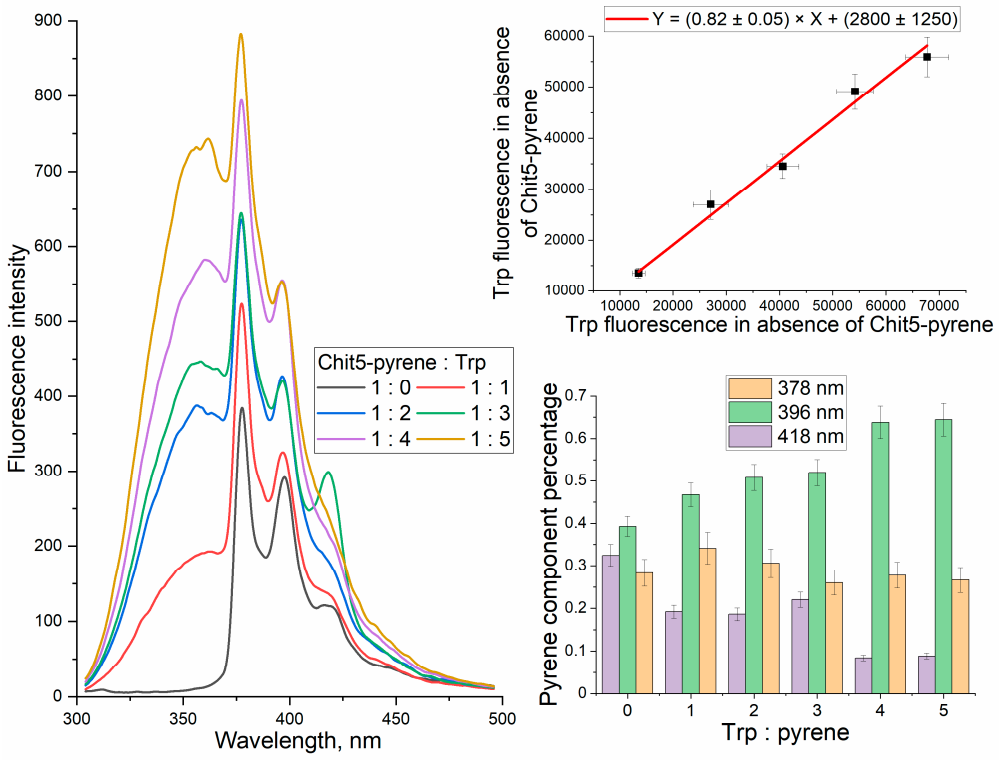

(a)

Preprints (www.preprints.org) | NOT PEER-REVIEWED | Posted: 22 June 2023 doi:10.20944/preprints202306.1629.v1

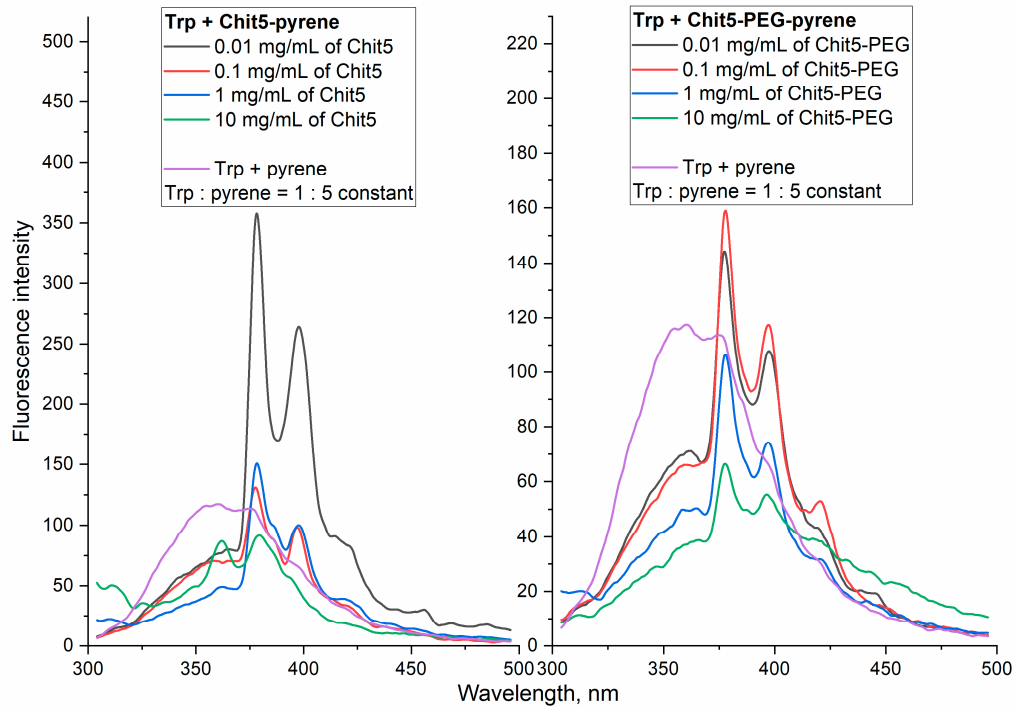

(b)

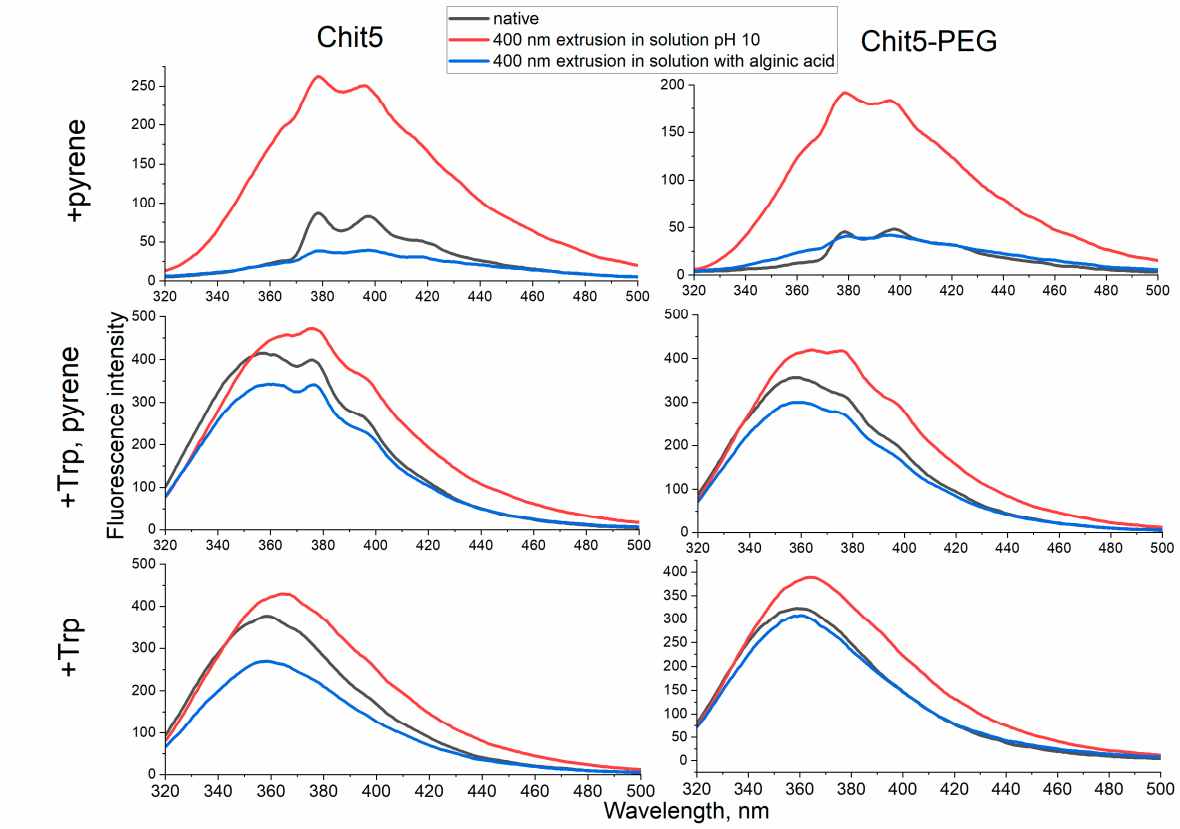

(c)

Figure 9. (a) The fluorescence spectra of Chit5-pyrene in the absence and in the presence of different concentrations of tryptophan, and the corresponding dependences of fluorescence integral intensities and percentages. (b) Fluorescence spectra of Chit5-pyrene, Chit5-PEG-pyrene, pyrene in the presence of tryptophan, depending on the concentration of the polymer. PBS (pH 7.4). (c) Fluorescence spectra of particles: Chit5, Chit5-PEG with pyrene (covalent), Trp or its mixture – native, 400 nm extrusion in solution with pH 10, 400 nm extrusion in solution with alginic acid. T = 40 °C.

 doi:10.20944/preprints202306.1629.v1

3.4.2. Ovalbumin as a model large molecule for drug delivery with FRET options

Volume-phase Macrogels

Ovalbumin is a 43 kDa protein, the main component of a chicken egg, which was selected as a model biomedically significant protein for encapsulation in the chitosan particles. The formation of ovalbumin-chitosan volume-phase gels is accompanied by the intensification of FRET between Tyr, Trp protein and pyrene in the polymer composition (Figure 10ab). With an increase in the concentration of the added protein to the pyrene-labeled chitosan, the proportion of the (400 nm) pyrene-component increases (green, Figure 10ab). At chitosan concentration of 0.05 mg/mL (below gel formation concentration), pyrene peaks strongly overlap with the peak of Trp emission in the protein, and at a concentration of 1 mg/ml (exceeding gel formation concentration), pyrene peaks are well resolved due to FRET. Thus, gelation is brightly manifested by FRET.

Nanogels

An important aspect for comparison of volume-phase gel and nanogel obtained by extrusion (with 400 nm membrane pores) and after washing of the particles (from soluble components by centrifugation (Figure 10c). It turned out that Chit5 at a concentration of 0.01 mg/mL after filtration does not form particles and exits through the pores. And at a concentration of 0.1 mg/mL and higher (up to 1 mg/mL), protein-chitosan nanoparticles (with pyrene fluorescence at $\lambda max \cong 375$ nm,) are formed. At the same time, Chit5-PEG forms protein-polymer particles at all the concentrations considered (0.01-1 mg/mL), which determines its potential for biomedical use as drug delivery systems or the creation of gel formulations.

FTIR spectroscopy studies of ovalbumin-chitosan interaction upon gelation.

FTIR provides valuable data on the molecular details of gelation and was used by us to confirm the fluorescence data. Figure 10d shows the FTIR spectra of ovalbumin in free form and in complex with chitosan particles. In the protein spectrum, the main absorption bands are: amide 1 (1600-1700 cm^{-1}, ν(C=O)) and amide 2 (1500-1600 cm^{-1}, δ(N–H)), ν (C–H) 2580-2970 cm^{-1}. In the spectrum of complex particles, a characteristic peak of oscillations of C-O bonds in Chit5-PEG appears, the shape of the ν(C-H) band changes and the intensity of the absorption bands of amide 1 and amide 2 decreases, which is associated with complexation and was shown by us earlier on concanavalin A [55,84–86].

Preprints (www.preprints.org) | NOT PEER-REVIEWED | Posted: 22 June 2023 doi:10.20944/preprints202306.1629.v1

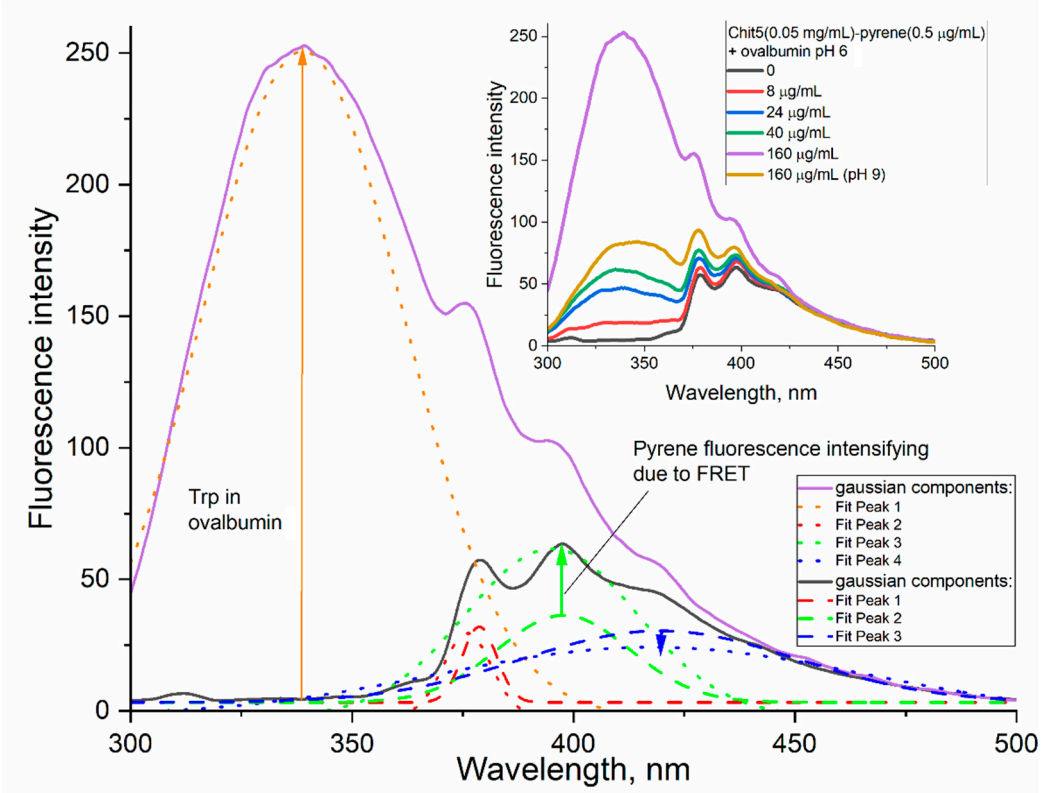

(a)

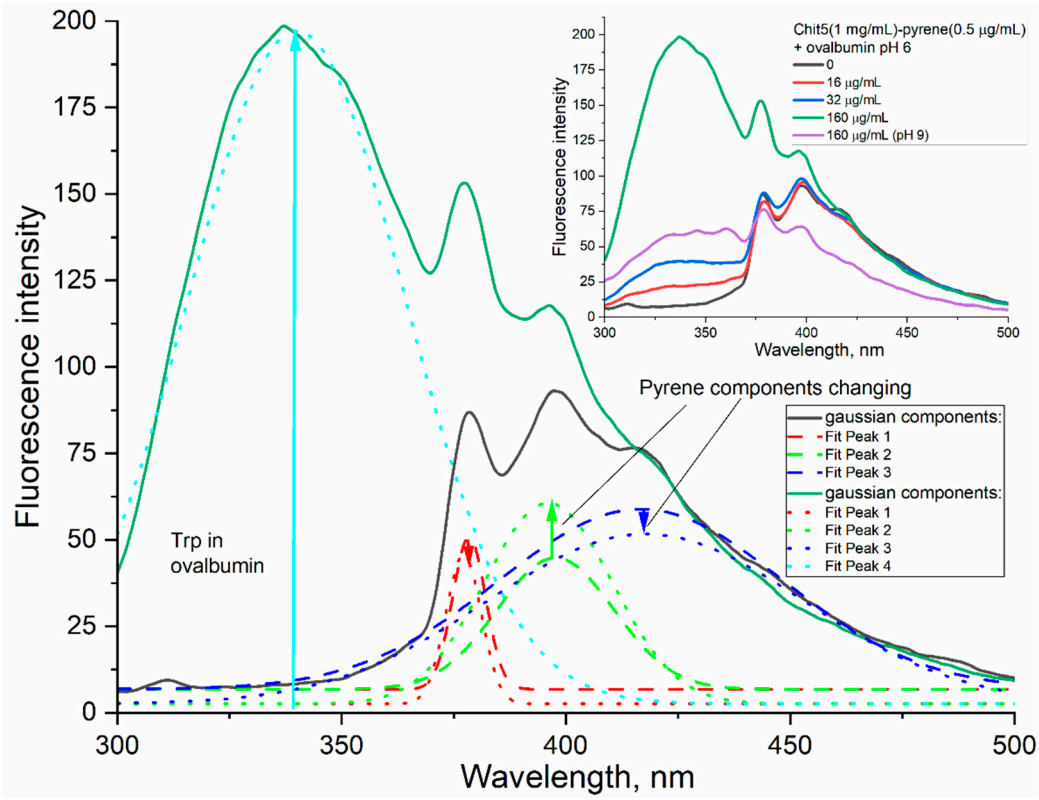

(b)

Preprints (www.preprints.org) | NOT PEER-REVIEWED | Posted: 22 June 2023 doi:10.20944/preprints202306.1629.v1

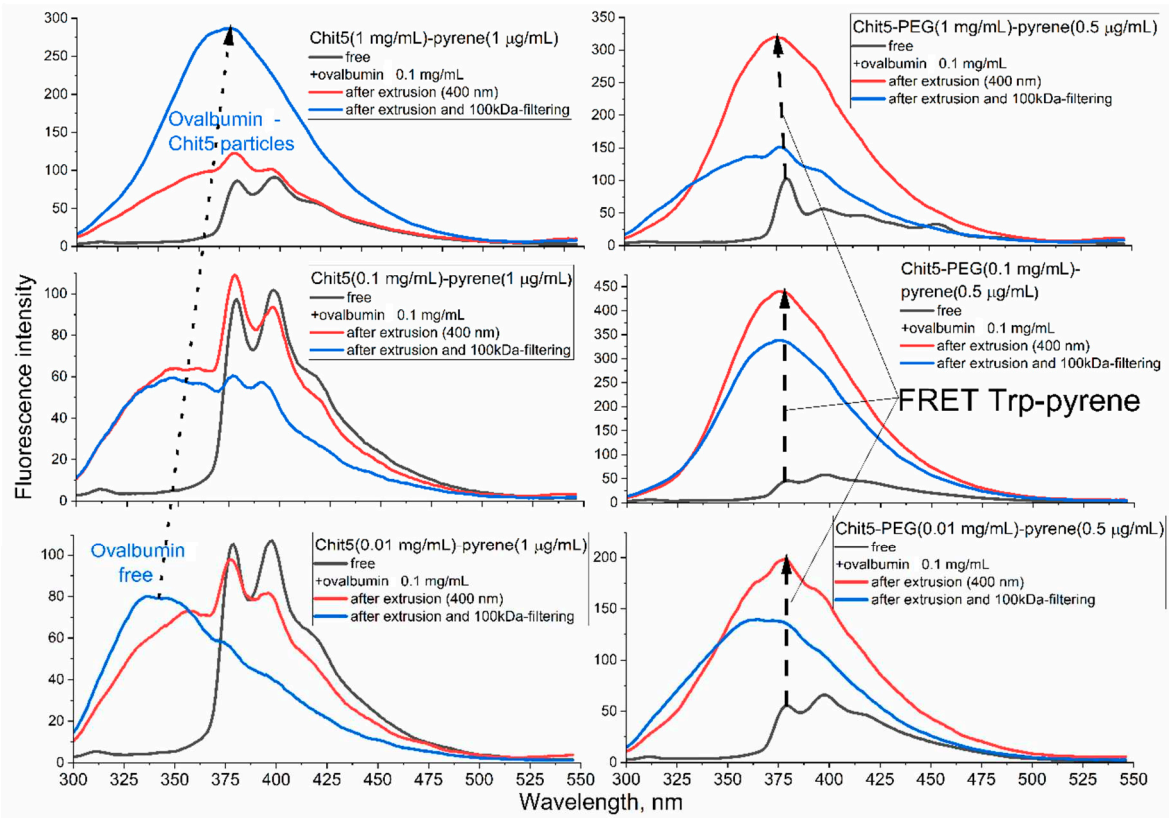

(c)

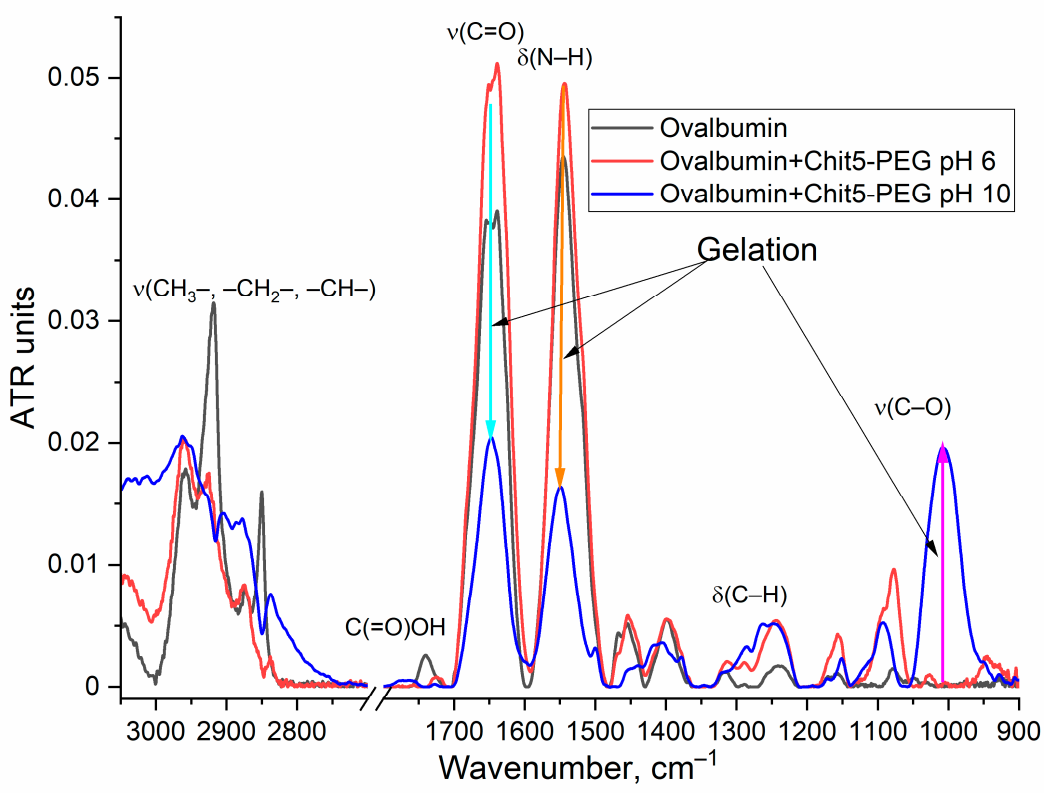

(d)

Preprints (www.preprints.org) | NOT PEER-REVIEWED | Posted: 22 June 2023 doi:10.20944/preprints202306.1629.v1

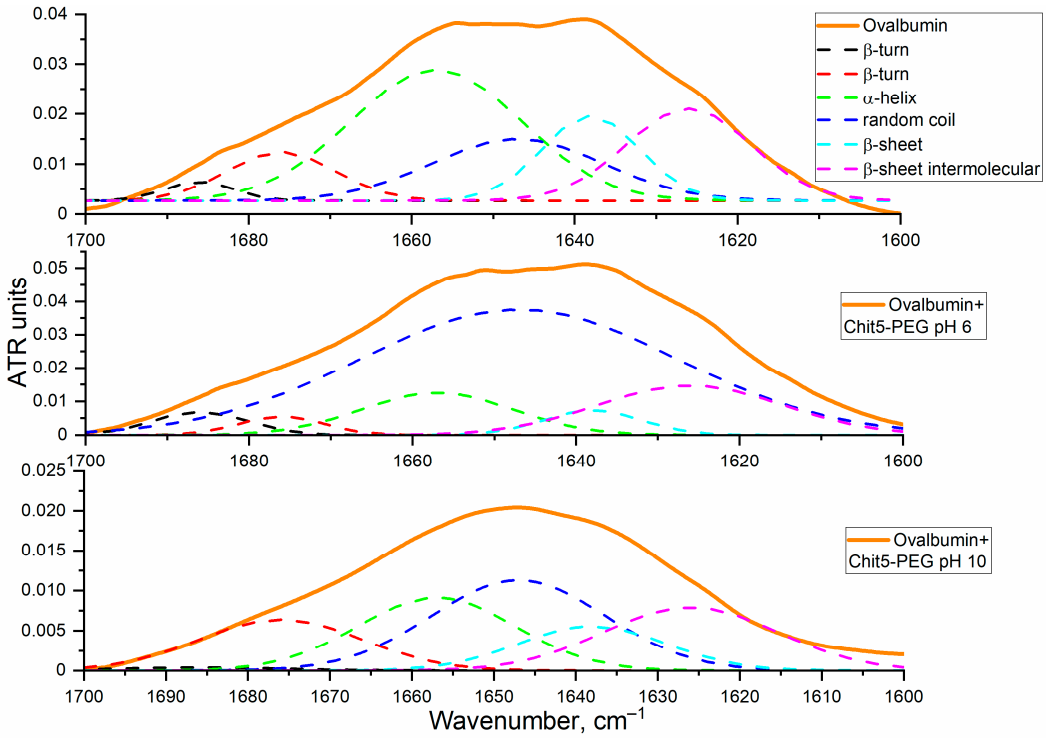

(e)

Figure 10. (a) The fluorescence spectra of Chit5-pyrene (0.05 mg/mL of Chit5, 0.5 μg/mL of pyrene) in the absence and in the presence of different concentrations of ovalbumin, and deconvolution of peaks with gaussians. (b) The fluorescence spectra of Chit5-pyrene (1 mg/mL of Chit5, 0.5 μg/mL of pyrene) in the absence and in the presence of different concentrations of ovalbumin, and deconvolution of peaks with gaussians. Phosphate buffer (10mM pH 6). Borate buffer (10mM pH 9). (c) The fluorescence spectra of particles formed by Chit5, Chit5-PEG alone (black) and after extrusion in borate buffer with pH 7.4 containing ovalbumin (red) or with subsequent centrifuge purification and separation of nanoparticles (blue). (d) FTIR spectra of ovalbumin free and ovalbumin-(Chit5-PEG) particles. (e) FTIR spectra deconvolution on followed components: 1638 cm^{-1} β-sheets, 1657 cm^{-1} α-helix, 1686 and 1676 cm^{-1} β -turns, 1626 - intermolecular β-sheets (aggregates). T = 40 °C.

The inclusion of ovalbumin in the particles of pegylated chitosan and protein gelation is accompanied by pronounced changes in the secondary structure (Figure 10e). 1638 cm^{-1} and 1657 cm^{-1} component intensities decrease when Chit5-PEG+ovalbumin particles are formed, which means that the proportion of β-sheet and α-helix decreases by 25% and 10% correspondingly, due to protein denaturation and the formation of disordered structures. Peak at 1624 cm^{-1} is increased, which corresponds to the formation of intermolecular aggregates (characteristic for ovalbumin), which was previously described in works on the properties of ovalbumin, adsorbed at the air-water interface [19,87,88]. Thus, ovalbumin is well incorporated in the chitosan particles, which follows from the aggregation of the protein upon chitosan particles formation and gelation. The property of gelation is promising for the creation of medicinal formulations, dietary supplements and thickeners in the food industry.

4. Conclusions

Particles based on chitosan and chitosan modified by PEG are of particular interest in aspects of the development of gels, medicinal formulations, as well as a biological additive for preventive and therapeutic feeding of animals. Optimization of the conditions for the formation of such particles and the selection of optimal parameters of nanoparticles and gels can be performed using fluorescent probes presented in this paper (pyrene, malachite green, congo red). Fluorophores abruptly ignite when nanoparticles are formed, and FRET is activated. According to the FRET phenomenon, it was shown that particles efficiently load both small drug molecules (on the tryptophan model) and large

ones (on the ovalbumin model). The fluorescent approach is quite accurate and highly sensitive to the microenvironment of the included drug molecule in nanoparticles. Original techniques for tracking gel formation are presented, which open up wide possibilities to find out the details of the formation of various molecular ensembles, for example, micelles from a new point of view and optimize existing particles with the potential for introduction into medicine and biotechnology. In addition, FTIR spectroscopy was used to elucidate the molecular details of the formation of ovalbumin-chitosan complexes accompanied by protein denaturation, aggregation and gel formation. The proposed polymers are effective as a broad-profile drug delivery system, and a narrow specialization of particles can be selected by varying the crosslinking conditions, pore sizes in the membrane, and monitoring the formation of particles using the methods developed by us.

Author Contributions: Conceptualization, E.V.K., I.D.Z; methodology, I.D.Z., E.V.K., I.V.S.; formal analysis, I.D.Z., I.V.S.; investigation, I.D.Z, I.V.S.; data curation, I.D.Z.; writing—original draft preparation, I.D.Z., I.V.S.; writing—review and editing, E.V.K; project supervision, E.V.K.; funding acquisition, E.V.K. All authors have read and agreed to the published version of the manuscript.

Institutional Review Board Statement: Not applicable.

Informed Consent Statement: Not applicable.

Data Availability Statement: The data presented in this study are available in the main text.

Funding: This research was funded by Russian Science Foundation, grant number 22-24-00604.

Acknowledgments: The work was performed using equipment of the program for the development of Moscow State University.

Conflicts of Interest: The authors declare no conflict of interest.

Abbreviations

Chit – chitosan

FRET – Förster resonance energy transfer

PEG – polyethyleneglycol

References

1. Morin-Crini, N.; Lichtfouse, E.; Torri, G.; Crini, G. Applications of chitosan in food, pharmaceuticals, medicine, cosmetics, agriculture, textiles, pulp and paper, biotechnology, and environmental chemistry. *Environ. Chem. Lett.* **2019**, *17*, 1667–1692, doi:10.1007/s10311-019-00904-x.
2. Moeini, A.; Pedram, P.; Makvandi, P.; Malinconico, M.; Gomez d'Ayala, G. Wound healing and antimicrobial effect of active secondary metabolites in chitosan-based wound dressings: A review. *Carbohydr. Polym.* **2020**, *233*, 115839, doi:10.1016/j.carbpol.2020.115839.
3. Bagheri, M.; Validi, M.; Gholipour, A.; Makvandi, P.; Sharifi, E. Chitosan nanofiber biocomposites for potential wound healing applications: Antioxidant activity with synergic antibacterial effect. *Bioeng. Transl. Med.* **2022**, *7*, 1–15, doi:10.1002/btm2.10254.
4. Riederer, M.S.; Requist, B.D.; Payne, K.A.; Way, J.D.; Krebs, M.D. Injectable and microporous scaffold of densely-packed, growth factor-encapsulating chitosan microgels. *Carbohydr. Polym.* **2016**, *152*, 792–801, doi:10.1016/j.carbpol.2016.07.052.
5. Jayakumar, R.; Chennazhi, K.P.; Muzzarelli, R.A.A.; Tamura, H.; Nair, S. V.; Selvamurugan, N. Chitosan conjugated DNA nanoparticles in gene therapy. *Carbohydr. Polym.* **2010**, *79*, 1–8, doi:10.1016/j.carbpol.2009.08.026.
6. V Thomas, L.; VG, R.; D Nair, P. Effect of stiffness of chitosan-hyaluronic acid dialdehyde hydrogels on the viability and growth of encapsulated chondrocytes. *Int. J. Biol. Macromol.* **2017**, *104*, 1925–1935, doi:10.1016/j.ijbiomac.2017.05.116.
7. Singh, P.; Medronho, B.; Alves, L.; da Silva, G.J.; Miguel, M.G.; Lindman, B. Development of carboxymethyl cellulose-chitosan hybrid micro- and macroparticles for encapsulation of probiotic bacteria. *Carbohydr. Polym.* **2017**, *175*, 87–95, doi:10.1016/j.carbpol.2017.06.119.
8. Mohamed, S.H.; Arafa, A.S.; Mady, W.H.; Fahmy, H.A.; Omer, L.M.; Morsi, R.E. Preparation and immunological evaluation of inactivated avian influenza virus vaccine encapsulated in chitosan nanoparticles. *Biologicals* **2018**, *51*, 46–53, doi:10.1016/j.biologicals.2017.10.004.

9. Hirano, S.; Itakura, C.; Seino, H.; Akiyama, Y.; Nonaka, I.; Kanbara, N.; Kawakami, T. Chitosan as an Ingredient for Domestic Animal Feeds. *J. Agric. Food Chem.* **1990**, *38*, 1214–1217, doi:10.1021/jf00095a012.
10. Abdel-Ghany, H.M.; Salem, M.E.S. Effects of dietary chitosan supplementation on farmed fish; a review. *Rev. Aquac.* **2020**, *12*, 438–452, doi:10.1111/raq.12326.
11. Whitacre, D.M. *Reviews of Environmental Contamination and Toxicology*; 2015; T. 233; ISBN 9783319104799.
12. Divya, K.; Jisha, M.S. Chitosan nanoparticles preparation and applications. *Environ. Chem. Lett.* **2018**, *16*, 101–112, doi:10.1007/s10311-017-0670-y.
13. Rahmanian-devin, P.; Rahimi, V.B.; Askari, V.R. 6640893.Pdf. **2021**, *2021*.
14. Calvo, P.; Remuñán-López, C.; Vila-Jato, J.L.; Alonso, M.J. Novel hydrophilic chitosan-polyethylene oxide nanoparticles as protein carriers. *J. Appl. Polym. Sci.* **1997**, *63*, 125–132, doi:10.1002/(SICI)1097-4628(19970103)63:1<125::AID-APP13>3.0.CO;2-4.
15. Maitra, A.; Ghosh, P.K.; De, T.K.; Sahoo, S.K. Process for the preparation of highly monodispersed polymeric hydrophilic nanoparticles. **1997**, 5.
16. Brunel, F.; Véron, L.; David, L.; Domard, A.; Delair, T. A novel synthesis of chitosan nanoparticles in reverse emulsion. *Langmuir* **2008**, *24*, 11370–11377, doi:10.1021/la801917a.
17. Positi v ely charged nanoparticles for impro v ing the oral bioa v ailability of cyclosporin-A. **2002**, *249*, 101–108.
18. Jayakumar, R.; Prabaharan, M.; Nair, S. V.; Tamura, H. Novel chitin and chitosan nanofibers in biomedical applications. *Biotechnol. Adv.* **2010**, *28*, 142–150, doi:10.1016/j.biotechadv.2009.11.001.
19. Kudryashova, E. V. Reversible self-association of ovalbumin at air-water interfaces and the consequences for the exerted surface pressure. *Protein Sci.* **2005**, *14*, 483–493, doi:10.1110/ps.04771605.
20. Caldera, F.; Tannous, M.; Cavalli, R.; Zanetti, M.; Trotta, F. Evolution of Cyclodextrin Nanosponges. *Int. J. Pharm.* **2017**, *531*, 470–479, doi:10.1016/j.ijpharm.2017.06.072.
21. Samal, S.K.; Dash, M.; Vlierberghe, S. Van; Kaplan, D.L.; Chiellini, E.; Blitterswijk, C. van; Moroni, L.; Dubruel, P. Cationic polymers and their therapeutic potential. *Chem. Soc. Rev.* **2012**, *41*, 7147–7194, doi:10.1039/c2cs35094g.
22. Lin, D.; Xiao, L.; Qin, W.; Loy, D.A.; Wu, Z.; Chen, H.; Zhang, Q. Preparation, characterization and antioxidant properties of curcumin encapsulated chitosan/lignosulfonate micelles. *Carbohydr. Polym.* **2022**, *281*, 119080, doi:10.1016/j.carbpol.2021.119080.
23. Bratskaya, S.; Skatova, A.; Privar, Y.; Boroda, A.; Kantemirova, E.; Maiorova, M.; Pestov, A. Stimuli-responsive dual cross-linked n-carboxyethylchitosan hydrogels with tunable dissolution rate. *Gels* **2021**, *7*, doi:10.3390/gels7040188.
24. Buranachai, T.; Praphairaksit, N.; Muangsin, N. Chitosan/polyethylene glycol beads crosslinked with tripolyphosphate and glutaraldehyde for gastrointestinal drug delivery. *AAPS PharmSciTech* **2010**, *11*, 1128–1137, doi:10.1208/s12249-010-9483-z.
25. Muzzarelli, R.A.A. Genipin-crosslinked chitosan hydrogels as biomedical and pharmaceutical aids. *Carbohydr. Polym.* **2009**, *77*, 1–9, doi:10.1016/j.carbpol.2009.01.016.
26. Bhattarai, N.; Ramay, H.R.; Gunn, J.; Matsen, F.A.; Zhang, M. PEG-grafted chitosan as an injectable thermosensitive hydrogel for sustained protein release. *J. Control. Release* **2005**, *103*, 609–624, doi:10.1016/j.jconrel.2004.12.019.
27. Ravishankar, K.; Dhamodharan, R. Advances in chitosan-based hydrogels: Evolution from covalently crosslinked systems to ionotropically crosslinked superabsorbents. *React. Funct. Polym.* **2020**, *149*, 104517, doi:10.1016/j.reactfunctpolym.2020.104517.
28. Manuscript, A. ce Ac us pt. **2019**, 0–5.
29. Fuenzalida, J.P.; Weikert, T.; Hoffmann, S.; Vila-Sanjurjo, C.; Moerschbacher, B.M.; Goycoolea, F.M.; Kolkenbrock, S. Affinity protein-based FRET tools for cellular tracking of chitosan nanoparticles and determination of the polymer degree of acetylation. *Biomacromolecules* **2014**, *15*, 2532–2539, doi:10.1021/bm500394v.
30. Lundin, M.; Blomberg, E.; Tilton, R.D. Polymer dynamics in layer-by-layer assemblies of chitosan and heparin. *Langmuir* **2010**, *26*, 3242–3251, doi:10.1021/la902968h.
31. Chuburu, F.; Malystkyi, V.; Moreau, J.; Callewaert, M.; Henoumont, C.; Cadiou, C.; Feuillie, C.; Laurent, S.; Molinari, M. Synthesis and Characterization of Conjugated Hyaluronic Acids. Application to Stability Studies of Chitosan-Hyaluronic Acid Nanogels Based on Fluorescence Resonance Energy Transfer. *Gels* **2022**, *8*, doi:10.3390/gels8030182.
32. Tammam, S.N.; Azzazy, H.M.E.; Breitinger, H.G.; Lamprecht, A. Chitosan Nanoparticles for Nuclear Targeting: The Effect of Nanoparticle Size and Nuclear Localization Sequence Density. *Mol. Pharm.* **2015**, *12*, 4277–4289, doi:10.1021/acs.molpharmaceut.5b00478.
33. Hoffmann, S.; Gorzelanny, C.; Moerschbacher, B.; Goycoolea, F.M. Physicochemical characterization of FRET-labelled chitosan nanocapsules and model degradation studies. *Nanomaterials* **2018**, *8*, doi:10.3390/nano8100846.

34. Liu, P.; Wang, R.; Su, W.; Qian, C.; Li, X.; Gao, L.; Jiao, T. Research advances in preparation and application of chitosan nanofluorescent probes. *Int. J. Biol. Macromol.* **2020**, *163*, 1884–1896, doi:10.1016/j.ijbiomac.2020.09.190.
35. Kinase, P. Quantitation of the Interaction. **1993**, 13310–13317.
36. Bastiaens, P.I.H.; Pap, E.H.W.; Borst, J.W.; van Hoek, A.; Kulinski, T.; Rigler, R.; Visser, A.J.W.G. The interaction of pyrene labeled diacylglycerol with protein kinase C in mixed micelles. *Biophys. Chem.* **1993**, *48*, 183–191, doi:10.1016/0301-4622(93)85009-7.
37. Tan, L.; Huang, R.; Li, X.; Liu, S.; Shen, Y.M.; Shao, Z. Chitosan-based core-shell nanomaterials for pH-triggered release of anticancer drug and near-infrared bioimaging. *Carbohydr. Polym.* **2017**, *157*, 325–334, doi:10.1016/j.carbpol.2016.09.092.
38. Harish, R.; Nisha, K.D.; Prabakaran, S.; Sridevi, B.; Harish, S.; Navaneethan, M.; Ponnusamy, S.; Hayakawa, Y.; Vinniee, C.; Ganesh, M.R. Cytotoxicity assessment of chitosan coated CdS nanoparticles for bio-imaging applications. *Appl. Surf. Sci.* **2020**, *499*, 143817, doi:10.1016/j.apsusc.2019.143817.
39. Shan, C.; Yang, H.; Han, D.; Zhang, Q.; Ivaska, A.; Niu, L. Graphene/AuNPs/chitosan nanocomposites film for glucose biosensing. *Biosens. Bioelectron.* **2010**, *25*, 1070–1074, doi:10.1016/j.bios.2009.09.024.
40. Kyzas, G.Z.; Bikiaris, D.N.; Mitropoulos, A.C. Chitosan adsorbents for dye removal: a review. *Polym. Int.* **2017**, *66*, 1800–1811, doi:10.1002/pi.5467.
41. Kim, H.C.; Park, W.H. Fluorescent property of glycol chitosan-fluorescein isothiocyanate conjugate for bio-imaging material. *Int. J. Biol. Macromol.* **2019**, *135*, 1217–1221, doi:10.1016/j.ijbiomac.2019.06.038.
42. Zhao, J.; Wu, J. Preparation and Characterization of the Fluorescent Chitosan Nanoparticle Probe. *Chinese J. Anal. Chem.* **2006**, *34*, 1555–1559, doi:10.1016/S1872-2040(07)60015-2.
43. Liu, J.; Zhang, L.; Wang, C.; Xu, H.; Zhao, X. Preparation and characterization of lectin-conjugated chitosan fluorescent nanoparticles. *Mol. Biosyst.* **2010**, *6*, 954–957, doi:10.1039/b927040j.
44. Zlotnikov, I.D.; Malashkeevich, S.M.; Belogurova, N.G.; Kudryashova, E. V. Thermoreversible Gels Based on Chitosan Copolymers as "Intelligent" Drug Delivery System with Prolonged Action for Intramuscular Injection. *Pharmaceutics* **2023**, *15*, doi:10.3390/pharmaceutics15051478.
45. Bhattarai, N.; Matsen, F.A.; Zhang, M. PEG-grafted chitosan as an injectable thermoreversible hydrogel. *Macromol. Biosci.* **2005**, *5*, 107–111, doi:10.1002/mabi.200400140.
46. Catanzano, O.; Gomez d'Ayala, G.; D'Agostino, A.; Di Lorenzo, F.; Schiraldi, C.; Malinconico, M.; Lanzetta, R.; Bonina, F.; Laurienzo, P. PEG-crosslinked-chitosan hydrogel films for in situ delivery of Opuntia ficus-indica extract. *Carbohydr. Polym.* **2021**, *264*, 117987, doi:10.1016/j.carbpol.2021.117987.
47. Yang, C.; Gao, S.; Dagnæs-Hansen, F.; Jakobsen, M.; Kjems, J. Impact of PEG Chain Length on the Physical Properties and Bioactivity of PEGylated Chitosan/siRNA Nanoparticles in Vitro and in Vivo. *ACS Appl. Mater. Interfaces* **2017**, *9*, 12203–12216, doi:10.1021/acsami.6b16556.
48. Prabaharan, M. Chitosan-based nanoparticles for tumor-targeted drug delivery. *Int. J. Biol. Macromol.* **2015**, *72*, 1313–1322, doi:10.1016/j.ijbiomac.2014.10.052.
49. Catanzano, O.; Gomez d'Ayala, G.; D'Agostino, A.; Di Lorenzo, F.; Schiraldi, C.; Malinconico, M.; Lanzetta, R.; Bonina, F.; Laurienzo, P. PEG-crosslinked-chitosan hydrogel films for in situ delivery of Opuntia ficus-indica extract. *Carbohydr. Polym.* **2021**, *264*, 117987, doi:10.1016/j.carbpol.2021.117987.
50. Mi, F.L.; Sung, H.W.; Shyu, S.S.; Su, C.C.; Peng, C.K. Synthesis and characterization of biodegradable TPP/genipin co-crosslinked chitosan gel beads. *Polymer (Guildf).* **2003**, *44*, 6521–6530, doi:10.1016/S0032-3861(03)00620-7.
51. López-León, T.; Carvalho, E.L.S.; Seijo, B.; Ortega-Vinuesa, J.L.; Bastos-González, D. Physicochemical characterization of chitosan nanoparticles: Electrokinetic and stability behavior. *J. Colloid Interface Sci.* **2005**, *283*, 344–351, doi:10.1016/j.jcis.2004.08.186.
52. Zlotnikov, I.D.; Streltsov, D.A.; Ezhov, A.A. Smart pH- and Temperature-Sensitive Micelles Based on Chitosan Grafted with Fatty Acids to Increase the Efficiency and Selectivity of Doxorubicin and Its Adjuvant Regarding the Tumor Cells. **2023**.
53. Zlotnikov, I.D.; Streltsov, D.A.; Belogurova, N.G.; Kudryashova, E. V. Chitosan or Cyclodextrin Grafted with Oleic Acid Self-Assemble into Stabilized Polymeric Micelles with Potential of Drug Carriers. *Life* **2023**, *13*, doi:10.3390/life13020446.
54. Zlotnikov, I.D.; Ezhov, A.A.; Vigovskiy, M.A.; Grigorieva, O.A.; Dyachkova, U.D.; Belogurova, N.G.; Kudryashova, E. V Application Prospects of FTIR Spectroscopy and CLSM to Monitor the Drugs Interaction with Bacteria Cells Localized in Macrophages for Diagnosis and Treatment Control of Respiratory Diseases. **2023**, 1–23.
55. Zlotnikov, I.D.; Kudryashova, E. V Spectroscopy Approach for Highly - Efficient Screening of Lectin - Ligand Interactions in Application for Mannose Receptor and Molecular Containers for Antibacterial Drugs. **2022**.
56. Le-Vinh, B.; Le, N.M.N.; Nazir, I.; Matuszczak, B.; Bernkop-Schnürch, A. Chitosan based micelle with zeta potential changing property for effective mucosal drug delivery. *Int. J. Biol. Macromol.* **2019**, *133*, 647–655, doi:10.1016/j.ijbiomac.2019.04.081.

57. Pereira, P.; Morgado, D.; Crepet, A.; David, L.; Gama, F.M. Glycol chitosan-based nanogel as a potential targetable carrier for siRNA. *Macromol. Biosci.* **2013**, *13*, 1369–1378, doi:10.1002/mabi.201300123.
58. Bhat, A.R.; Wani, F.A.; Behera, K.; Khan, A.B.; Patel, R. Formulation of biocompatible microemulsions for encapsulation of anti-TB drug rifampicin: A physicochemical and spectroscopic study. *Colloids Surfaces A Physicochem. Eng. Asp.* **2022**, *645*, 128846, doi:10.1016/j.colsurfa.2022.128846.
59. Bonferoni, M.C.; Sandri, G.; Dellera, E.; Rossi, S.; Ferrari, F.; Mori, M.; Caramella, C. Ionic polymeric micelles based on chitosan and fatty acids and intended for wound healing. Comparison of linoleic and oleic acid. *Eur. J. Pharm. Biopharm.* **2014**, *87*, 101–106, doi:10.1016/j.ejpb.2013.12.018.
60. Mohr, A.; Talbiersky, P.; Korth, H.G.; Sustmann, R.; Boese, R.; Bläser, D.; Rehage, H. A new pyrene-based fluorescent probe for the determination of critical micelle concentrations. *J. Phys. Chem. B* **2007**, *111*, 12985–12992, doi:10.1021/jp0731497.
61. Ollmann, M.; Galla, H.J.; Schwarzmann, G.; Sandhoff, K. Pyrene-Labeled Gangliosides: Micelle Formation in Aqueous Solution, Lateral Diffusion, and Thermotropic Behavior in Phosphatidylcholine Bilayers. *Biochemistry* **1987**, *26*, 5943–5952, doi:10.1021/bi00392a055.
62. Berghmans, M.; Govaers, S.; Berghmans, H.; De Schryver, F.C. Study of polymer gelation by fluorescence spectroscopy. *Polym. Eng. Sci.* **1992**, *32*, 1466–1470, doi:10.1002/pen.760322004.
63. Fluksman, A.; Benny, O. A robust method for critical micelle concentration determination using coumarin-6 as a fluorescent probe. *Anal. Methods* **2019**, *11*, 3810–3818, doi:10.1039/c9ay00577c.
64. Liow, S.S.; Dou, Q.; Kai, D.; Karim, A.A.; Zhang, K.; Xu, F.; Loh, X.J. Thermogels: In Situ Gelling Biomaterial. *ACS Biomater. Sci. Eng.* **2016**, *2*, 295–316, doi:10.1021/acsbiomaterials.5b00515.
65. Branca, C.; Khouzami, K.; Wanderlingh, U.; D'Angelo, G. Effect of intercalated chitosan/clay nanostructures on concentrated pluronic F127 solution: A FTIR-ATR, DSC and rheological study. *J. Colloid Interface Sci.* **2018**, *517*, 221–229, doi:10.1016/j.jcis.2018.02.004.
66. Zlotnikov, I.D.; Ezhov, A.A.; Ferberg, A.S.; Krylov, S.S.; Semenova, M.N.; Semenov, V. V; Kudryashova, E. V Polymeric Micelles Formulation of Combretastatin Derivatives with Enhanced Solubility , Cytostatic Activity and Selectivity against Cancer Cells. **2023**.
67. Lu, Y.J.; Lan, Y.H.; Chuang, C.C.; Lu, W.T.; Chan, L.Y.; Hsu, P.W.; Chen, J.P. Injectable thermo-sensitive chitosan hydrogel containing CPT-11-loaded EGFR-targeted graphene oxide and SLP2 shRNA for localized drug/gene delivery in glioblastoma therapy. *Int. J. Mol. Sci.* **2020**, *21*, 1–29, doi:10.3390/ijms21197111.
68. Wu, J.; Su, Z.; Ma, G. A thermo- and pH-sensitive hydrogel composed of quaternized chitosan / glycerophosphate. **2006**, *315*, 1–11, doi:10.1016/j.ijpharm.2006.01.045.
69. Mohamed, N.A.; Abd El-Ghany, N.A. Synthesis and antimicrobial activity of some novel terephthaloyl thiourea cross-linked carboxymethyl chitosan hydrogels. *Cellulose* **2012**, *19*, 1879–1891, doi:10.1007/s10570-012-9789-y.
70. Eivazzadeh-Keihan, R.; Radinekiyan, F.; Maleki, A.; Salimi Bani, M.; Hajizadeh, Z.; Asgharnasl, S. A novel biocompatible core-shell magnetic nanocomposite based on cross-linked chitosan hydrogels for in vitro hyperthermia of cancer therapy. *Int. J. Biol. Macromol.* **2019**, *140*, 407–414, doi:10.1016/j.ijbiomac.2019.08.031.
71. Dobryakova, N. V.; Zhdanov, D.D.; Sokolov, N.N.; Aleksandrova, S.S.; Pokrovskaya, M. V.; Kudryashova, E. V. Improvement of Biocatalytic Properties and Cytotoxic Activity of L-Asparaginase from Rhodospirillum rubrum by Conjugation with Chitosan-Based Cationic Polyelectrolytes. *Pharmaceuticals* **2022**, *15*, doi:10.3390/ph15040406.
72. Gao, J.Q.; Zhao, Q.Q.; Lv, T.F.; Shuai, W.P.; Zhou, J.; Tang, G.P.; Liang, W.Q.; Tabata, Y.; Hu, Y.L. Gene-carried chitosan-linked-PEI induced high gene transfection efficiency with low toxicity and significant tumor-suppressive activity. *Int. J. Pharm.* **2010**, *387*, 286–294, doi:10.1016/j.ijpharm.2009.12.033.
73. Kievit, F.M.; Veiseh, O.; Bhattarai, N.; Fang, C.; Gunn, J.W.; Lee, D.; Ellenbogen, R.G.; Olson, J.M.; Zhang, M. PEI-PEG-chitosan-copolymer-coated iron oxide nanoparticles for safe gene delivery: Synthesis, complexation, and transfection. *Adv. Funct. Mater.* **2009**, *19*, 2244–2251, doi:10.1002/adfm.200801844.
74. Jiang, H.L.; Kim, Y.K.; Arote, R.; Nah, J.W.; Cho, M.H.; Choi, Y.J.; Akaike, T.; Cho, C.S. Chitosan-graft-polyethylenimine as a gene carrier. *J. Control. Release* **2007**, *117*, 273–280, doi:10.1016/j.jconrel.2006.10.025.
75. Ping, Y.; Liu, C.; Zhang, Z.; Liu, K.L.; Chen, J.; Li, J. Chitosan-graft-(PEI-β-cyclodextrin) copolymers and their supramolecular PEGylation for DNA and siRNA delivery. *Biomaterials* 2011, *32*, 8328–8341.
76. Jiang, H.L.; Kim, Y.K.; Arote, R.; Jere, D.; Quan, J.S.; Yu, J.H.; Choi, Y.J.; Nah, J.W.; Cho, M.H.; Cho, C.S. Mannosylated chitosan-graft-polyethylenimine as a gene carrier for Raw 264.7 cell targeting. *Int. J. Pharm.* **2009**, *375*, 133–139, doi:10.1016/j.ijpharm.2009.03.033.
77. Vasile, C.; Pamfil, D.; Stoleru, E.; Baican, M. New developments in medical applications of hybrid hydrogels containing natural polymers. *Molecules* **2020**, *25*, 1–68, doi:10.3390/molecules25071539.
78. Zhou, X.; Su, F.; Lu, H.; Senechal-Willis, P.; Tian, Y.; Johnson, R.H.; Meldrum, D.R. An FRET-based ratiometric chemosensor for in vitro cellular fluorescence analyses of pH. *Biomaterials* **2012**, *33*, 171–180, doi:10.1016/j.biomaterials.2011.09.053.

79. Zhong, H.; Liu, C.; Ge, W.; Sun, R.; Huang, F.; Wang, X. Self-Assembled Conjugated Polymer/Chitosan-graft-Oleic Acid Micelles for Fast Visible Detection of Aliphatic Biogenic Amines by «turn-On» FRET. *ACS Appl. Mater. Interfaces* **2017**, *9*, 22875–22884, doi:10.1021/acsami.7b06168.
80. Dennis, A.M.; Rhee, W.J.; Sotto, D.; Dublin, S.N.; Bao, G. Quantum dot-fluorescent protein fret probes for sensing intracellular pH. *ACS Nano* **2012**, *6*, 2917–2924, doi:10.1021/nn2038077.
81. Chen, T.; He, B.; Tao, J.; He, Y.; Deng, H.; Wang, X.; Zheng, Y. Application of Förster Resonance Energy Transfer (FRET) technique to elucidate intracellular and In Vivo biofate of nanomedicines. *Adv. Drug Deliv. Rev.* 2019, *143*, 177–205.
82. Huebsch, N.D.; Mooney, D.J. Fluorescent resonance energy transfer: A tool for probing molecular cell-biomaterial interactions in three dimensions. *Biomaterials* **2007**, *28*, 2424–2437, doi:10.1016/j.biomaterials.2007.01.023.
83. Ghezzi, M.; Pescina, S.; Padula, C.; Santi, P.; Del Favero, E.; Cantù, L.; Nicoli, S. Polymeric micelles in drug delivery: An insight of the techniques for their characterization and assessment in biorelevant conditions. *J. Control. Release* **2021**, *332*, 312–336, doi:10.1016/j.jconrel.2021.02.031.
84. Zlotnikov, I.D.; Vigovskiy, M.A.; Davydova, M.P.; Danilov, M.R.; Dyachkova, U.D.; Grigorieva, O.A.; Kudryashova, E. V Mannosylated Systems for Targeted Delivery of Antibacterial Drugs to Activated Macrophages. **2022**, 1–29.
85. Zlotnikov, I.D.; Ezhov, A.A.; Petrov, R.A.; Vigovskiy, M.A.; Grigorieva, O.A.; Belogurova, N.G.; Kudryashova, E. V. Mannosylated Polymeric Ligands for Targeted Delivery of Antibacterials and Their Adjuvants to Macrophages for the Enhancement of the Drug Efficiency. *Pharmaceuticals* **2022**, *15*, 1172, doi:10.3390/ph15101172.
86. Zlotnikov, I.D.; Kudryashova, E. V. Mannose Receptors of Alveolar Macrophages as a Target for the Addressed Delivery of Medicines to the Lungs. *Russ. J. Bioorganic Chem.* **2022**, *48*, 46–75, doi:10.1134/S1068162022010150.
87. Kudryashova, E. V.; Meinders, M.B.J.; Visser, A.J.W.G.; Van Hoek, A.; De Jongh, H.H.J. Structure and dynamics of egg white ovalbumin adsorbed at the air/water interface. *Eur. Biophys. J.* **2003**, *32*, 553–562, doi:10.1007/s00249-003-0301-3.
88. Dong, A.; Meyer, J.D.; Brown, J.L.; Manning, M.C.; Carpenter, J.F. Comparative fourier transform infrared and circular dichroism spectroscopic analysis of α1-proteinase inhibitor and ovalbumin in aqueous solution. *Arch. Biochem. Biophys.* **2000**, *383*, 148–155, doi:10.1006/abbi.2000.2054.